

Utah State University

DigitalCommons@USU

All Graduate Theses and Dissertations, Spring
1920 to Summer 2023

Graduate Studies

5-2016

ATP Usage in the Dark-Operative Protochlorophyllide Oxidoreductase

Mark S. Soffe
Utah State University

Follow this and additional works at: <https://digitalcommons.usu.edu/etd>

 Part of the [Other Chemistry Commons](#)

Recommended Citation

Soffe, Mark S., "ATP Usage in the Dark-Operative Protochlorophyllide Oxidoreductase" (2016). *All Graduate Theses and Dissertations, Spring 1920 to Summer 2023*. 4753.
<https://digitalcommons.usu.edu/etd/4753>

This Thesis is brought to you for free and open access by the Graduate Studies at DigitalCommons@USU. It has been accepted for inclusion in All Graduate Theses and Dissertations, Spring 1920 to Summer 2023 by an authorized administrator of DigitalCommons@USU. For more information, please contact digitalcommons@usu.edu.



ATP USAGE IN THE DARK-OPERATIVE PROTOCHLOROPHYLLIDE
OXIDOREDUCTASE

by

Mark S. Soffe

A thesis submitted in partial fulfillment
of the requirements for the degree

of

MASTER OF SCIENCE

in

Biochemistry

Approved:

Dr. Edwin Antony
Major Professor

Dr. Korry Hintze
Committee Member

Dr. Lance Seefeldt
Committee Member

Dr. Mark McLellan
Vice President for Research and
Dean of the School of Graduate Studies

UTAH STATE UNIVERSITY
Logan, Utah

2016

Copyright © Mark Soffe 2016

All Rights Reserved

ABSTRACT

ATP Usage in the Dark-operative Protochlorophyllide Oxidoreductase

by

Mark S. Soffe, Master of Science

Utah State University, 2016

Major Professor: Dr. Edwin Antony
Department: Biochemistry

Photosynthesis is a fundamental biological process that sustains life on earth. Chlorophyll is the pigment that captures sunlight and converts it to chemical energy through photosynthesis. These essential light-harvesting compounds are found in photosynthetic plants, cyanobacteria, green algae, angiosperms and gymnosperms. In the chlorophyll biosynthetic pathway, protochlorophyllide (Pchl_{id}) serves as the precursor molecule for chlorophyll. Protochlorophyllide oxidoreductases are a class of enzymes that catalyze the conversion of Pchl_{id} to chlorophyllide *a* (Chl_{id}), which subsequently is reduced and modified to form chlorophyll. A light-dependent protochlorophyllide oxidoreductase (LPOR) is found in flowering plants (angiosperms), and as the name suggests, requires the energy from light to catalyze the conversion. An unrelated dark-operative light-independent version (DPOR - dark-operative protochlorophyllide oxidoreductase) is found in cyanobacteria, photosynthetic bacteria, green algae and gymnosperms. DPOR functions in the absence of light, or low-light conditions and in the absence of oxygen. DPOR is a multi-subunit complex consisting of the BchL, BchN and

BchB proteins which share striking structural similarities to the Nif proteins in the nitrogenase complex. ATP binding and hydrolysis is an essential aspect of DPOR catalysis, though it still remains mysterious as to how the energy from ATP is used to drive substrate reduction. The role of ATP in the conversion of Pchlide to Chlide has been examined kinetically to establish when ATP is hydrolyzed in the catalytic mechanism. Additionally, variants of the BchL protein have been developed to include a functional linked BchL homodimer, as well as Walker A mutated forms on one, or both ATPase sites of the protein. The data suggest a dynamic mechanism in which the binding and hydrolysis of both ATP are required for normal function.

(82 pages)

PUBLIC ABSTRACT

ATP Usage in the Dark-operative Protochlorophyllide Oxidoreductase

Mark S. Soffe

Chlorophylls are essential pigment molecules that function in photosynthesis, and serve to aid in utilizing energy from sunlight to power cellular processes in plants, and other organisms. To make chlorophyll, photosynthetic organisms devote an abundance of resources and energy to ensure their appropriate construction. This process of making chlorophylls is highlighted by the penultimate step in the pathway—the conversion of protochlorophyllide (Pchl_{id}) to chlorophyllide *a* (Chl_{id}).

This conversion can be mediated in two different ways, depending on the type of organism. The first method incorporates the use of a light-activated system called the light-dependent protochlorophyllide oxidoreductase (LPOR). This system, as the name suggests, uses light to trigger the production of chlorophylls for use in photosynthesis. The focus of research provided hereafter is centered on a structurally unrelated dark-operative system (DPOR), which generates chlorophyll in the absence of light, or in low-light conditions.

DPOR is structurally related to the enzyme nitrogenase, which functions to reduce atmospheric nitrogen into a form usable for living systems to incorporate into their metabolism. Both DPOR and nitrogenase are similar in that both require ATP binding and hydrolysis for electron transfer to occur, but differ in that DPOR is a much slower enzyme. Even though ATPase activity is essential for catalysis, the role of ATP

throughout the catalytic mechanism is not well understood. The research contained herein was conducted in order to better characterize the role of ATP in DPOR during this critical step in chlorophyll production.

When comparing steady-state rates between DPOR and nitrogenase, DPOR was found to perform 400-fold slower with respect to ATPase activity. However, the initial rates of ATP hydrolysis were found to be very similar, indicating that the two systems are divergent after the initial hydrolysis occurs. Mutational studies further show that both ATPase sites are required for normal function.

CONTENTS

	Page
ABSTRACT.....	iii
PUBLIC ABSTRACT	v
LIST OF FIGURES	ix
CHAPTER	
I. INTRODUCTION	1
REFERENCES	13
II. ISOLATION OF DPOR COMPONENTS AND CHARACTERIZATION OF WILD-TYPE ACTIVITY	15
2.1 INTRODUCTION	15
2.2 METHODS	18
Cloning of DPOR Components – L-Protein	18
Cloning of DPOR Components – NB-Protein	19
Expression and Cluster Formation of the L-Protein	20
Growth and Expression of the NB-Protein	22
Purification of DPOR Components	24
Generation and Extraction of Pchlde.....	26
Pchlde Reduction Endpoint Assay	27
DPOR Steady-state ATPase Kinetics	28
Preliminary Pre-steady state Analysis of DPOR Activity	29
2.3 RESULTS	30
Cloning and Expression of DPOR Components from <i>E. coli</i>	30
Steady-state ATPase Analysis and Pchlde Reduction of DPOR.....	31
Pre-steady state Analysis of the L-Protein Catalyzed ATPase Cycle.....	34
2.4 DISCUSSION.....	39
ATP Hydrolysis Occurs Slowly in the Steady State.....	40
Preliminary Pre-steady State Data Suggest Rapid-burst ATP Hydrolysis on One Half of the DPOR Complex	41
REFERENCES	44
III. CONSTRUCTION OF LINKED L-PROTEIN CONSTRUCTS TO INVESTIGATE ATP-RELATED DYNAMICS.....	45
3.1 INTRODUCTION	45

3.2 METHODS	50
Plasmid Construction of the Homodimeric Linked L-Protein.....	50
Site-directed Mutagenesis and Construction of the K44A Walker A Mutant L-Proteins	52
Expression and Cluster Formation of the Homodimeric Linked L-Protein ...	53
Growth and Cluster Formation of the Homodimeric Non-Linked Walker A Mutant L-Protein	55
Expression and Cluster Formation of the Heterodimeric Linked Walker A Mutant L-Protein	56
Purification of the L-Protein Variants	57
Tev Protease Cleavage of the Homodimeric Linked L-Protein and Pchlide Reduction Endpoint Assays.....	59
Real-time Pchlide Kinetic Assay Using the Homodimeric Linked L-Protein....	61
3.3 RESULTS	62
Cloning and Expression of L-Protein Variants.....	62
The Homodimeric Linked L-Protein Behaves Similarly to the Wild-type Construct	63
The Walker A L-Protein Mutants Are Incapable of Substrate Reduction.....	64
3.4 DISCUSSION.....	64
REFERENCES	68
SUMMARY AND FUTURE WORK	69
REFERENCES	72

LIST OF FIGURES

Figure	Page
1.1 Chlorophyll biosynthesis pathway	3
1.2 Comparison of DPOR to nitrogenase and cofactor visualization	7
1.3 Representation of single electron cycle events for the L-Protein	10
2.1 Strategy and purification of BchL	32
2.2 Cloning strategy and purification of the BchNB protein	33
2.3 Pchl _a reduction assay using isolated DPOR components	35
2.4 Steady-state analysis of DPOR ATPase activity	37
2.5 Pre-steady state kinetic characterization of DPOR	38
3.1 Walker A motif in BchL from <i>Rhodobacter sphaeroides</i>	48
3.2 List of L-Protein constructs and their protein architecture	49
3.3 Depiction of purified L-Protein variants by SDS-PAGE	63
3.4 Qualitative Pchl _a reduction scans	65
3.5 Wild-type BchL and homodimeric linked L-protein reduction kinetics	66

CHAPTER I INTRODUCTION

Photosynthesis Importance and Overview of Chlorophylls

Photosynthesis is a critical biological process used by plants and other organisms which converts light energy into chemical energy. The complex series of chemical reactions are not only responsible for supplying oxygen to the atmosphere by means of carbon fixation, but also serve to produce essential organic compounds that help maintain life. Such a gargantuan task requires specialized components capable of mediating these energy transfer events. There have been years' worth of research dedicated to understanding how each of these components works together to produce, from seemingly impossible raw material sources such as molecular H₂O and CO₂—metabolic waste for some organisms, into higher value compounds that make life possible.

Central to the process of photosynthesis is chlorophyll. Chlorophylls are essential pigments that help to make photosynthesis possible by capturing light energy and directing it to reaction centers designed to make such energy conversion possible. Many different varieties of chlorophyll are used among photosynthetic bacteria, green algae, angiosperms, and gymnosperms, which are all used in the capture and conversion of light energy. Chlorophylls are porphyrin-containing pigments that are coordinated by a central magnesium ion, and are substituted variously in order to alter the electronics of the ring structure, affecting its absorptive properties. To localize their effect in photosynthesis, as well as to protect the organism from excessive oxidative damage, chlorophylls are found

attached, usually by means of carotenoids¹ to protein components which are found embedded in chloroplast membranes. Because of their structural complexity, and their importance in photosynthesis, Chlorophylls have a very long and dedicated synthetic pathway.

Synthetic Pathway of Chlorophyll, Leading to Protochlorophyllide a

Chlorophyll is one of the most abundant organic molecules on Earth. It is estimated that in a single leaf, assuming 70 million cells, houses about 600 million molecules of chlorophyll². Therefore, the requirement and synthesis of chlorophyll for use in photosynthesis is by no means trivial—in fact, the process of generating active chlorophyll requires enzymatic transformation involving fifteen distinct intermediates (Figure 1.1) beginning with the amino acid L-glutamate via the C5 pathway, which operates in the chloroplast³. The glutamate amino acid, interestingly, is converted to the aminoacyl-tRNA by glutamate-tRNA synthetase prior to being reduced by an NADPH-dependent glutamate-tRNA reductase to form the immediate precursor to 5-aminolevulinate, which becomes the primary building block to form the porphyrin ring of the chlorophyll⁴.

Where the first steps of chlorophyll synthesis tend to differ from that of non-photosynthetic organisms, the assembly of the porphyrin ring at least tends to follow more conventional transformation. The generated 5-aminolevulinate undergo additional transformation by 5-aminolevulinic acid dehydratase, which catalyzes asymmetric condensation of two molecules of 5-aminolevulinate. This completes the synthesis of one

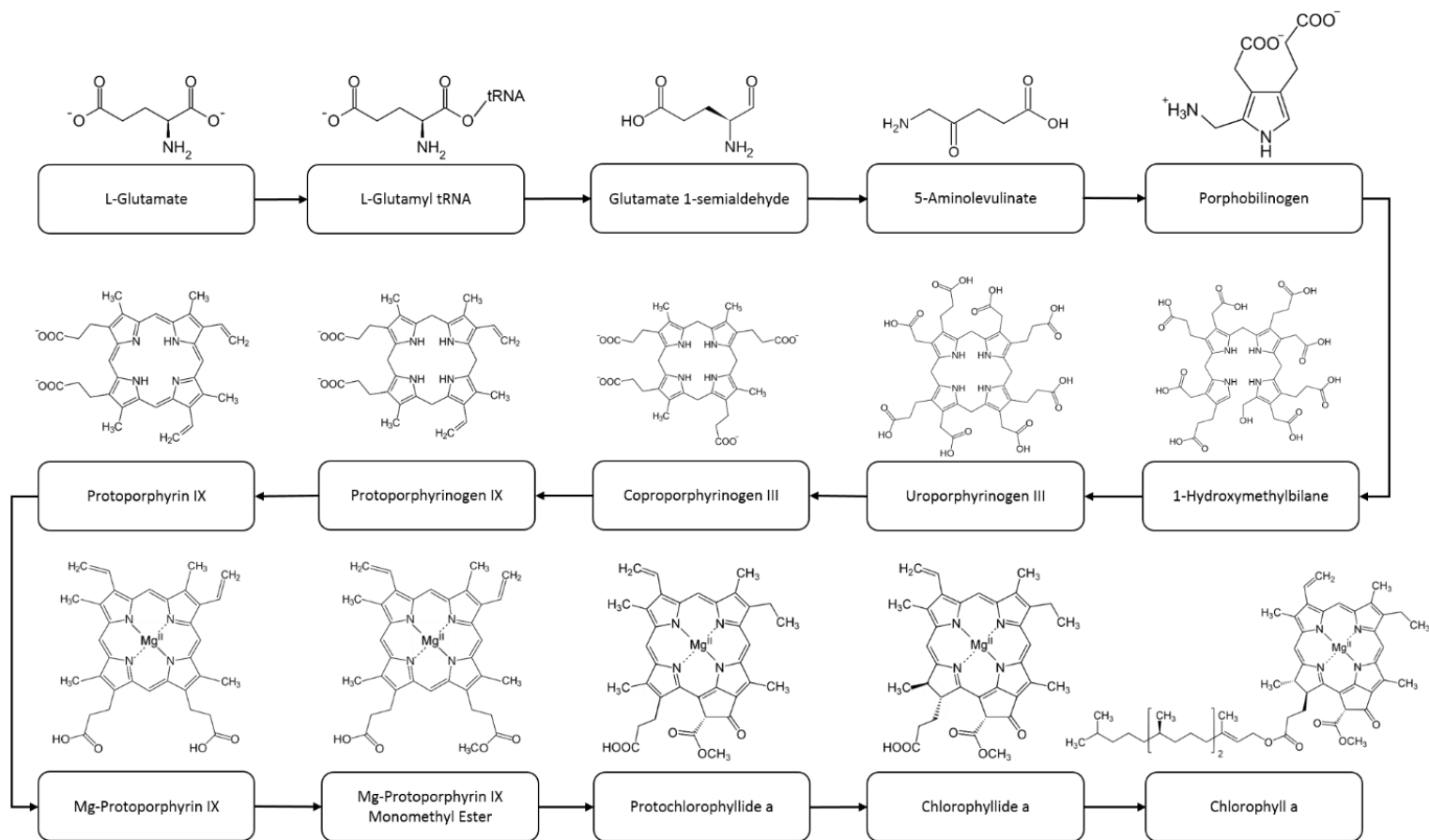


Figure 1.1. Chlorophyll biosynthesis pathway. The chlorophyll biosynthesis pathway starts with the substrate L-glutamate, where it is linked to tRNA by means of the enzyme glutamyl-tRNA synthetase and using Mg-ATP to become glutamyl tRNA. Reduction occurs to yield the semialdehyde glutamate precursor before it is enzymatically converted into 5-aminolevulinate, which serves as the building block of the porphyrin ring. The penultimate step in the pathway, the conversion of Pchlide to Chlide is mediated by either a light-dependent oxidoreductase (LPOR) or a light-independent DPOR.

of what will end up being four pyrrole rings in the completed porphyrin structure of chlorophyll⁵. Following the synthesis of individual pyrrole rings, four such components are linked together by porphobilinogen deaminase, which includes high sequence similarity among various organisms in its catalytic and substrate binding residues³. Uroporphyrinogen synthase follows up this transformation by closing the porphyrin ring. Following the completion of the porphyrin ring, it must be substituted correctly to gain the appropriate electronic properties required in the capture and conversion of light energy. Uroporphyrinogen III decarboxylase replaces acetic acid side chains with one-carbon methyl groups, coproporphyrinogen III oxidase transforms two propionic acid side chains into vinyl groups, and finally protoporphyrinogen IX oxidase, a flavoprotein, oxidizes the porphyrin to allow for absorption in the red region of the visible spectrum³.

From the intermediate protoporphyrin IX and on, the enzymes utilized are specific in the chlorophyll synthesis pathway. The process starts with the insertion of a Mg^{2+} ion by Mg-Chelatase⁶. Following addition of the central Mg^{2+} ion, the Mg-protoporphyrin monomethyl ester intermediate is formed by a methyltransferase that esterifies a propionic acid in order to form a fifth ring which is characteristic of active chlorophyll, then is reduced to yield protochlorophyllide a. Interestingly, the reduction of protochlorophyllide a (Pchlde) to Chlorophyllide a (Chlide), the immediate precursor for chlorophyll a, seems to be a key step in chlorophyll synthesis and its regulation, and will receive particular consideration.

DPOR and LPOR—Twin Models of Protochlorophyllide Reduction

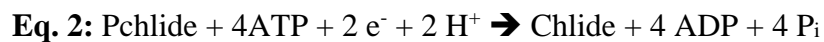
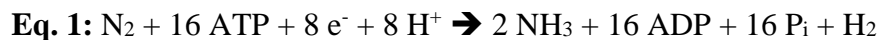
The transformation of Pchlide into Chlide is a stereospecific reduction of the C17=C18 double bond in ring IV of the porphyrin. This is the rate-limiting step in the biosynthetic pathway⁷. In addition to this, there is significant control related to the accumulation of Pchlide in angiosperms. To protect themselves from reactive oxygen species (ROS) damage resulting from the over-accumulation of free Pchlide, flowering plants have developed a mechanism to shut off synthesis of 5-aminolevulinate after a threshold amount of Pchlide is reached when grown under dark conditions, where the accumulated substrate is bound to a light-activated NADPH:Pchlide oxidoreductase, otherwise referred to as LPOR¹. Upon the addition of light, the substrate can be turned over to form Chlide by using NADPH as an electron source for the two electron reduction, and the addition of a proton by an adjacent tyrosine residue⁸. After this conversion takes place, Chlide may be used as a substrate to finally become chlorophyll a.

Angiosperms are completely reliant on this light-activated mechanism of chlorophyll synthesis, having only LPOR to perform the chemistry to convert Pchlide into Chlide. However, gymnosperms, algae, and cyanobacteria utilize an unrelated dark-operative system for the purpose of reducing Pchlide, known as the dark-operative protochlorophyllide oxidoreductase (DPOR) in addition to the light-active system. Anoxygenic photosynthetic bacteria such as *Rhodobacter capsulatus* and *Rhodobacter sphaeroides* are completely reliant on the dark-operative method which functions in the absence of light, and in the absence of oxygen. There are many reasons why this protein

is interesting to study, which include its similarity to nitrogenase, as well as the role ATP plays in the reaction mechanism.

DPOR Components and Similarity to Nitrogenase

While DPOR and LPOR both perform the same chemistry to reduce Pchlide to Chlide, it is both structurally and functionally different from LPOR. DPOR is a multi-protein complex comprised of two symmetrical catalytic halves containing the proteins BchL, BchN, and BchB. Each of these proteins share similarities with the Fe protein (NifH) and the MoFe protein (NifDK) of nitrogenase, both in functionality and in subunit and cofactor orientation. Nitrogenase is responsible for catalyzing the reduction of molecular dinitrogen to ammonia, which consumes 16 ATP and produces one obligate equivalent of hydrogen gas in eight total single-electron transfer cycles⁹ (Eq. 1). During catalysis, the association and dissociation of the Fe protein to the catalytic MoFe protein is coupled to the binding and hydrolysis of ATP, which also results in the transfer of electrons, one at a time, to metal centers that contribute to substrate reduction¹⁰. The same complex orientation and dynamics are achieved in DPOR for the purposes of catalysis¹¹, though DPOR catalyzes the two electron reduction of the C17=C18 double bond on Pchlide, which only requires two single-electron transfer cycles and the hydrolysis of 4 ATP (eq. 2).



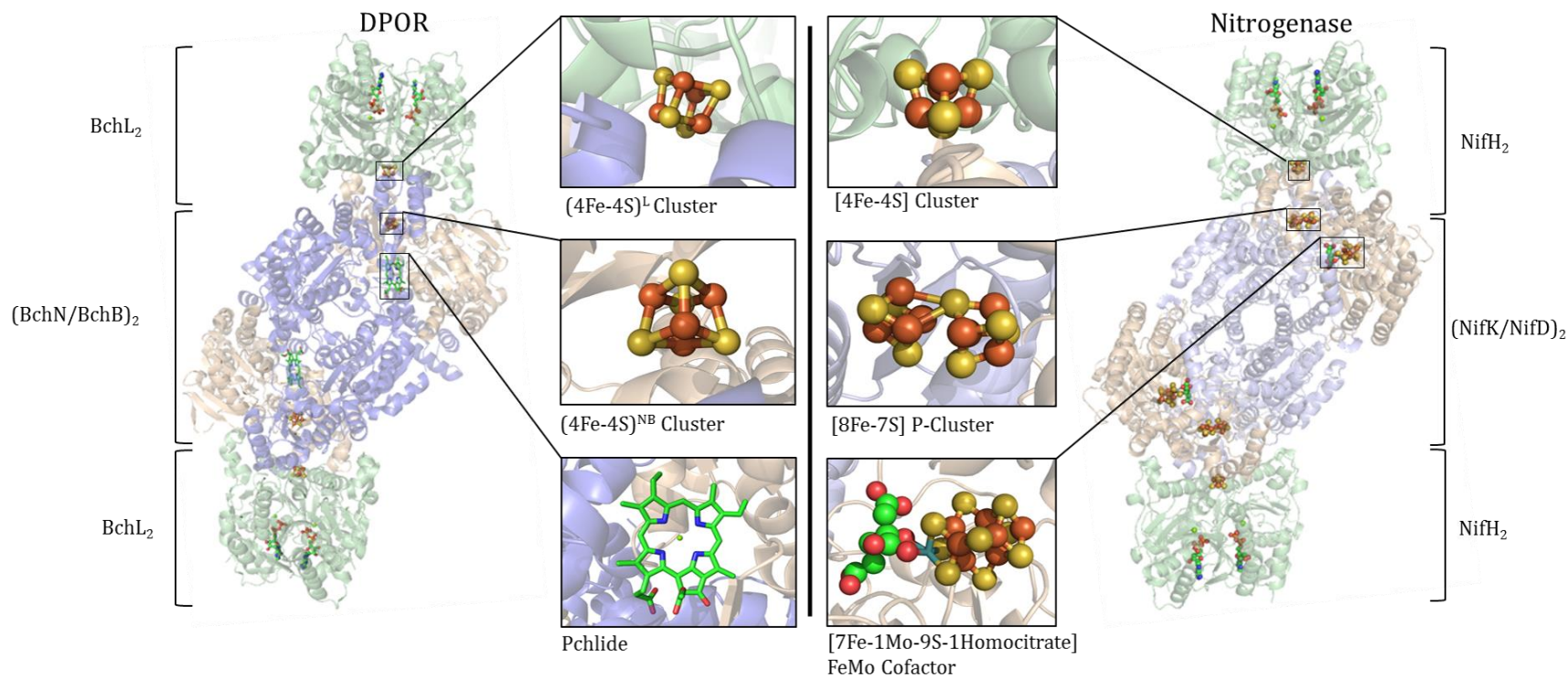


Figure 1.2. Comparison of DPOR to nitrogenase and cofactor visualization. DPOR and nitrogenase show considerable similarity to each other. Their similar subunit orientation and cofactor location may point to key architectural features that are conducive to reducing stable multiple bond systems, such as those found in dinitrogen and in conjugated porphyrin systems.

The BchN/BchB proteins of DPOR form a heterotetramer analogous to the MoFe protein of nitrogenase. However, there is no conservation in sequence between the two sites of substrate reduction, indicating differences in composition. The MoFe protein contains a unique [1Mo-7Fe-9S-1homocitrate] FeMo cofactor which serves as the site for dinitrogen reduction, whereas the NB-protein does not contain a metal cluster at the site of Pchlide reduction. The cofactor composition also varies greatly between the two systems (Figure 1.2). It can be purposed that the similarity in cofactor arraignment may produce an ideal architecture for an environment suited to reducing stable multiple-bond systems. Nitrogenase, in addition to the FeMo cofactor, also contains an [8Fe-7S] P-cluster, whereas the NB-protein only contains one [4Fe-4S] cluster that is uniquely ligated by one aspartate and three cysteine residues¹².

BchL is a homodimeric protein that is found at each end of the symmetrical complex of DPOR and functions to deliver electrons, one at a time, to the NB-protein in order to generate Chlide. This electron transfer is coupled to the binding and hydrolysis of two ATP per electron that is transferred. The L-protein shows significant structural and functional similarities to the Fe-protein of nitrogenase¹³—in fact, when looking at the amino acid sequence, BchL is about 30% identical and 50% similar to the Fe protein¹⁴, with the highest instances of similarity occurring in the ATP-binding motifs and the interface that coordinates with the [4Fe-4S] cluster that is joined symmetrically at the surface of the dimer¹⁴. Interestingly, the [4Fe-4S] cluster of the L-protein appears to be either less accessible, or is more reliant upon a large conformational change upon the binding of nucleotide than that of the Fe-protein due to the rate of chelation by α,α' -

dipyridal solution¹³. It is also worth noting that even with the high degree of similarity between the two proteins, and considering their identical function, they are not interchangeable for use in the alternative enzymatic system due to significant differences in surface charge used in recognition to the appropriate protein-protein interaction partner¹³.

Detailed Insights into the Chemistry of DPOR

With both the similarity to nitrogenase, and recent structural and inhibition studies to probe DPOR function^{11, 15}, detailed information has been gained about the reaction mechanism and chemistry of DPOR. Since Both DPOR and nitrogenase both utilize ATP-dependent single-electron donating proteins, by necessity, there needs to be a cycle (Figure 1.3) which accounts for association, electron transfer, ATP hydrolysis¹⁶, dissociation of the spent iron-protein, reduction of oxidized protein, and re-association of reduced protein to begin the cycle again. As it stands, there has not been much research performed to date that addresses the complexity of this single-electron transfer cycle, and the role that ATP plays in the dynamics at work. Mixed in with these steps, the DPOR mechanism also needs to include steps for substrate binding, transfer of a single electron from the NB cluster to Pchlide, proton addition, transfer of a second electron from NB to Pchlide coupled to a subsequent proton addition, and finally the release of Chlide¹⁵. The formation of the DPOR complex is essential for the successful reduction of substrate. From structural data^{11, 17, 18}, a number of key residues play important roles to maintain appropriate protein-protein interactions, cluster environment, and substrate orientation. The Cys95 residue in BchB seems to play a vital role in forming the NB complex.

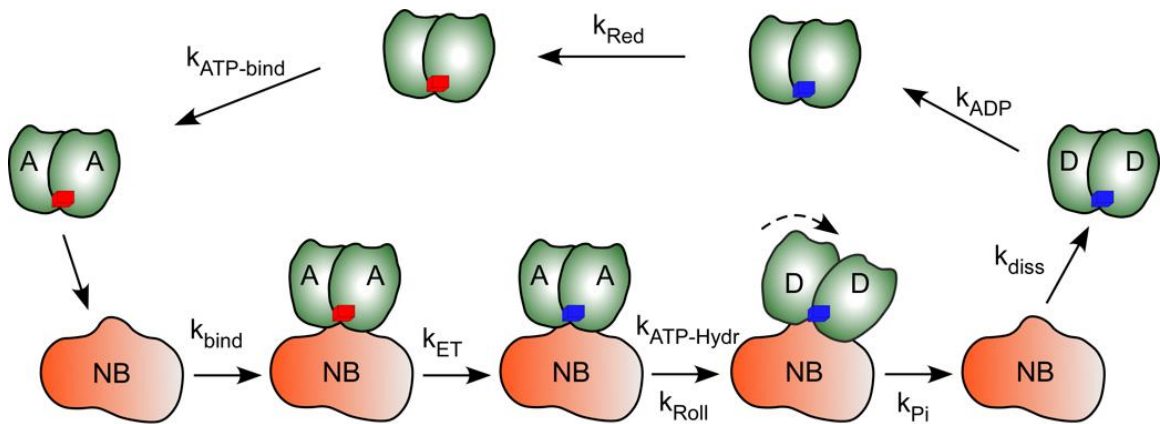


Figure 1.3. Representation of single electron cycle events for the L-protein.

The L-protein does not statically interact with the NB-protein. Rather, the DPOR complex is a dynamic fluctuation between oxidized and reduced, and L-protein bound and dissociated states. A single turn in the L-protein single electron cycle requires the binding of ATP to the L-protein, binding of L to the NB-protein, transfer of one electron coupled to the hydrolysis of both ATP, dissociation of L-protein, dissociation of ADP from the L-protein, reduction of the [4Fe-4S] cluster, and the binding again of ATP to the L-protein in preparation of the cycle repeating.

When mutated to alanine, not only did the enzyme lose ability to reduce Pchlide, but the protein-protein interaction between BchN and BchB was interrupted¹¹. Asp36 in BchB also plays a critical role in the appropriate assembly of the DPOR complex. While it has no effect on complex assembly, this residue is critical in coordination with the [4Fe-4S] NB cluster, which is uniquely ligated by three cysteines contributed by both BchN and BchB, as well as the aforementioned aspartic acid residue^{11, 17, 18}. When mutated to cysteine or alanine, while the ability to form a conventionally ligated [4Fe-4S] cluster was maintained, almost all reductive capability was lost. The cysteine and serine mutations completely abolished activity, while the alanine mutation significantly reduced

the activity to only 13% of the wild-type protein¹¹. This may indicate that the Asp36 ligation is required for appropriate flexibility of the NB-cluster to effectively maintain the correct orientation to reduce substrate. The shortest distance from the NB-cluster to Pchl_a is 10.0 Å, which supports through space electron transfer to be possible¹⁹. Phe25 of BchN also contributes to a suitable environment for electron transfer to the substrate^{11, 17}.

Fujita and his research team propose a trans-specific mechanism in which proton attack occurs sequentially and in opposite directions perpendicular to the porphyrin plane^{11, 20}. The H⁺ donors in the reaction are a BchB'-Asp274 residue that interestingly is located on the protein to which the opposite Pchl_a is bound, and the propionate side chain on the Pchl_a molecule itself. Rationale for identifying these groups as the H⁺ donors include their proximity (4.9 Å and 4.8 Å respectively) to the C17=C18 double bond of Pchl_a, as well as the distorted conformation of the propionate side chain illuminated by the structural data¹¹ which places it almost perpendicular to the porphyrin plane. Evidence for the trans-addition of H⁺ during electron transfer is found by observing the spatial arrangement of the H⁺ donors when Pchl_a is bound. Both the accuracy of the donors and the importance of the propionate conformation are supported in mutation studies of the BchB'-Asp274, where substrate reduction was lost upon change to an alanine, and by switching to the similar, but unnatural substrate chlorophyll c. Where chlorophyll a has a flexible propionate side chain, chlorophyll c has a rigid acrylate group which does not allow for the distorted conformation seen in the crystal

structure. Complete substrate reduction is not observed when chlorophyll c is used as substrate, where it acts as a competitive inhibitor for DPOR^{11, 20}.

Substrate reduction in DPOR is unique, and differs from what is observed in nitrogenase. Because of the absence of metal clusters at the site of substrate reduction, and the transfer of only one electron at a time by the L-protein, by necessity, substrate radicals are formed. In enzymes that normally produce radicals as reaction intermediates, such as B12 enzymes²¹ or radical SAM enzymes²², the radical that is generated is on its cofactor, and not on the substrate itself. DPOR has been found not only to generate substrate radicals during catalysis²⁰, but that the electrons, as well as the protons are added sequentially. This means that during catalysis, the first intermediate formed, confirmed by EPR, is an anion radical species of Pchlide. One proton from the propionate side chain is used to resolve the charge, making a neutral radical intermediate. The second electron transferred to substrate forms a lone pair on C17 of the Chlide intermediate species, forming an anion intermediate, which is eventually resolved by the donation of the second H⁺ from BchB'-Asp274. When chlorophyll c is used as a substrate, only an anion radical is generated²⁰.

Rationale for Master's Thesis Research

While there have been studies on DPOR concerning its role in chlorophyll biosynthesis, and its relation to nitrogenase, there are still important questions that remain mysterious. Namely, how does DPOR use the energy from hydrolyzing two ATP to accomplish electron transfer? Or, what dynamics and regulatory elements are observed in

the L-protein upon hydrolysis by its dual ATPase sites during the catalytic cycle? This investigation seeks to address these questions.

1. The components of DPOR were expressed and purified using the *E. coli* expression system for the purpose of *in vitro* characterization of the enzyme.
2. Assays were developed to examine its ability to reduce Pchlide and hydrolyze ATP
3. Novel linked constructs of the L-protein were designed to examine dynamics of the dual ATPase sites, as well as to determine functionality in various conditions
4. How mutations in the Walker-A motif in one or both of the ATPase sites affect the ability of the L-protein to hydrolyze ATP, and ultimately reduce Pchlide.

REFERENCES

1. Reinbothe, S., Reinbothe, C., Apel, K., Lebedev, N. Evolution of chlorophyll biosynthesis--the challenge to survive photooxidation. *Cell* **86** (5), 703-5 (1996).
2. Simpson, D. J., Laboratory, C., Knoetzel, J., Bremen, U. o. Light-harvesting Complexes of Plants and Algae: Introduction, Survey and Nomenclature. 493-506 (2015).
3. Von Wettstein, D., Gough, S., Kannangara, C. G. Chlorophyll Biosynthesis. *Plant Cell* **7** (7), 1039-1057 (1995).
4. Kannangara, C. G., Andersen, R. V., Pontoppidan, B., Willows, R., von Wettstein, D. Enzymic and mechanistic studies on the conversion of glutamate to 5-aminolaevulinate. *Ciba Found Symp* **180**, 3-20; discussion 21-5 (1994).
5. Jordan, P. M., Chapter 1 The biosynthesis of 5-aminolaevulinic acid and its transformation into uroporphyrinogen III. **19**, 1-66 (1991).
6. Bauer, C. E., Bollivar, D. W., Suzuki, J. Y. Genetic analyses of photopigment biosynthesis in eubacteria: a guiding light for algae and plants. *J Bacteriol* **175** (13), 3919-25 (1993).

7. Masuda, T., Fujita, Y. Regulation and evolution of chlorophyll metabolism. *Photochem Photobiol Sci* **7** (10), 1131-49 (2008).
8. Schoefs, B., Franck, F. Protochlorophyllide Reduction: Mechanisms and Evolution¶. [http://dx.doi.org/10.1562/0031-8655\(2003\)0782.0.CO;2](http://dx.doi.org/10.1562/0031-8655(2003)0782.0.CO;2) (2009).
9. Godje, O., Peyerl, M., Seebauer, T., Lamm, P., Mair, H., Reichart, B., Armstrong, G. A. Greening in the dark: light-independent chlorophyll biosynthesis from anoxygenic photosynthetic bacteria to gymnosperms. (1998).
10. Rees, D. C., Howard, J. B. Nitrogenase: standing at the crossroads. *Curr Opin Chem Biol* **4** (5), 559-66 (2000).
11. Muraki, N., Nomata, J., Ebata, K., Mizoguchi, T., Shiba, T., Tamiaki, H., Kurisu, G., Fujita, Y. X-ray crystal structure of the light-independent protochlorophyllide reductase. *Nature* **465** (7294), 110-4 (2010).
12. Terada, T., Hirabayashi, K., Liu, D., Nakamura, T., Wakimoto, T., Matsumoto, T., Tatsumi, K. [3:1] site-differentiated [4Fe-4S] clusters having one carboxylate and three thiolates. *Inorg Chem* **52** (20), 11997-2004 (2013).
13. Sarma, R., Barney, B. M., Hamilton, T. L., Jones, A., Seefeldt, L. C., Peters, J. W. Crystal structure of the L protein of *Rhodobacter sphaeroides* light-independent protochlorophyllide reductase with MgADP bound: a homologue of the nitrogenase Fe protein. *Biochemistry* **47** (49), 13004-15 (2008).
14. Suzuki, J. Y., Bauer, C. E. Light-independent chlorophyll biosynthesis: involvement of the chloroplast gene chlL (frxC). *Plant Cell* **4** (8), 929-40 (1992).
15. Nomata, J., Kondo, T., Itoh, S., Fujita, Y. Nicotinamide is a specific inhibitor of dark-operative protochlorophyllide oxidoreductase, a nitrogenase-like enzyme, from *Rhodobacter capsulatus*. *FEBS Lett* **587** (18), 3142-7 (2013).
16. Duval, S., Danyal, K., Shaw, S., Lytle, A. K., Dean, D. R., Hoffman, B. M., Antony, E., Seefeldt, L. C. Electron transfer precedes ATP hydrolysis during nitrogenase catalysis. *Proc Natl Acad Sci U S A* **110** (41), 16414-9 (2013).
17. Reinbothe, C. Chlorophyll biosynthesis: spotlight on protochlorophyllide reduction. *Trends in Plant Science* **15** (11), 614-624 (2010).
18. Moser, J., Lange, C., Krausze, J., Rebelein, J., Schubert, W. D., Ribbe, M. W., Heinz, D. W., Jahn, D. Structure of ADP-aluminium fluoride-stabilized protochlorophyllide oxidoreductase complex. *Proc Natl Acad Sci U S A* **110** (6), 2094-8 (2013).
19. Page, C. C., Moser, C. C., Chen, X., Dutton, P. L. Natural engineering principles of electron tunnelling in biological oxidation-reduction. *Nature* **402** (6757), 47-52 (1999).
20. Nomata, J., Kondo, T., Mizoguchi, T., Tamiaki, H., Itoh, S., Fujita, Y. Dark-operative protochlorophyllide oxidoreductase generates substrate radicals by an iron-sulphur cluster in bacteriochlorophyll biosynthesis. *Sci Rep* **4**, 5455 (2014).
21. Dowling, D. P., Croft, A. K., Drennan, C. L. Radical use of Rossmann and TIM barrel architectures for controlling coenzyme B12 chemistry. *Annu Rev Biophys* **41**, 403-27 (2012).
22. Shisler, K. A., Broderick, J. B. Emerging themes in radical SAM chemistry. *Curr Opin Struct Biol* **22** (6), 701-10 (2012).

CHAPTER II

ISOLATION OF DPOR COMPONENTS AND CHARACTERIZATION OF WILD-TYPE ACTIVITY

2.1 INTRODUCTION

DPOR represents a critical step in the synthesis of chlorophyll for use in the capture and conversion of light energy during photosynthesis. It is a multi-subunit complex that consists of the catalytic BchN/BchB $\alpha 2/\beta 2$ heterotetramer, and the homodimeric BchL protein. During catalysis, Pchl_{ide} binds to the NB-protein and awaits electrons to be delivered by the L-protein, one at a time, in a process that is dependent upon the binding and hydrolysis of two ATP. Pchl_{ide} reduction has been well characterized in previous studies. The K_m value for Pchl_{ide} is 10.6 μM from enzyme obtained from *Rhodobacter capsulatus*¹. Under *in vitro* conditions where the flux of L-protein:NB-protein was held at or higher than 3:1, the specific activity of DPOR from *Rhodobacter capsulatus*² was found to be 26.2 nmol_{Chlide} minute⁻¹ mg⁻¹. DPOR is also unique with respect to its method used to reduce Pchl_{ide}. It is one of a handful of enzymes that forms substrate radicals, coupled with sequential, stereospecific proton addition that first generates a neutral radical on the chlorin ring itself, then produces an carbanion intermediate that is resolved by the addition of a second proton³.

The DPOR catalyzed reduction of Pchl_{ide} mechanistically resembles nitrogenase catalysis⁴ in that both enzymatic systems share significant topological homology with

respect to subunit orientation. Like nitrogenase, DPOR contains oxygen-sensitive metal clusters required for catalysis⁵ but may be expressed and isolated from an *E. coli* expression system, and does not require the control of a complex operon such as the *nif* operon that functions to control appropriate expression and assembly of proteins that are required to maintain nitrogenase for nitrogen fixation.

Nitrogenase is a difficult enzyme to study, partly due to the fact that it must be expressed in a diazotroph system, such as in *Azotobacter vinelandii*, under control of the *nifH* operon⁶. DPOR is more convenient to study due to its ability to be expressed in an *E. coli* expression system. While its expression and purification have been accomplished previously⁷, it's worth noting that the production of protein controlled by IPTG induction in *E. coli* not only overexpresses each component of DPOR, but also ensures proper saturation with iron-sulfur clusters necessary for catalytic activity. The cloning strategy used to obtain each component of DPOR will be discussed hereafter, also noting how Pchlide is obtained for use during *in vitro* characterization of the purified components.

While there has been substantial characterization of DPOR with respect to Pchlide reduction, there are certain aspects of the catalytic mechanism that remain mysterious. Recent pre-steady state studies in the nitrogenase system have revealed some interesting characteristics in the process of nitrogen fixation. Namely, obtaining first-order rate constants for the principle steps of electron transfer, ATP hydrolysis, Phosphate (P_i) release, and Fe-protein dissociation during the single-electron transfer cycle have revealed several interesting insights⁸. First, electron transfer was found to precede ATP hydrolysis by the Fe-protein, showing that it is the free energy of ATP binding and that of

the protein-protein interaction between the Fe-protein and the MoFe protein that orchestrates electron transfer, and not ATP hydrolysis. Second, the two symmetrical halves of nitrogenase may work in a sequential manner, in that the activity on one half of the protein may allosterically control essential events to occur on the other catalytic half.

Because of the significant homology between DPOR and nitrogenase with respect to subunit orientation and the dependence on ATP to mediate essential catalytic events, these insights may also hold true in DPOR and other nitrogenase-like reductases. To date, the molecular basis for such allosteric coupling is not understood in such enzymatic systems, and DPOR function could reveal additional common mechanistic insights. Additionally, the role of ATP has not been well characterized for this enzymatic system. Therefore, the following studies were performed with the goal of addressing these issues. In order to achieve such understanding, molecular biology techniques were used to isolate the DPOR components from *E. coli*, and *in vitro* assays were developed to characterize wild-type DPOR activity. A combination of steady-state and pre-steady state kinetics techniques were used to observe nuances in the catalytic mechanism of DPOR, which, other than rudimentary analysis with respect to Pchlide reduction, is not well understood. The ATPase ability of the system was also observed in the same manner. These studies and the resulting data show that DPOR can be expressed and purified from an *E. coli* expression system, and that the resulting isolated components are occupied with stoichiometric amounts of iron consistent with the [4Fe-4S] clusters necessary for catalysis. DPOR, like nitrogenase, is capable of substrate reduction in an ATP-dependent manner, albeit this reduction occurs much slower—on the order of 400 fold. Preliminary

pre-steady state ATPase data show that DPOR behaves like nitrogenase, in that two ATP are initially hydrolyzed at a burst-rate of 73 second^{-1} , which is 900 times faster than the steady state activity. The stoichiometric amount hydrolyzed may provide support for a similar allosteric model of activity between the two symmetrical halves. This chapter details the initial purification and characterization of wild-type DPOR activity.

2.2 METHODS

Cloning of DPOR Components – L-Protein

A plasmid was designed using RSF-duet as a parent vector to carry the BchL gene (Figure 2.1). Expression is controlled by the *lac* operon, upon addition of IPTG. The *BchL* gene from *Rhodobacter sphaeroides* was first amplified using PCR. The primer with sequence 5' ATT TAA GGA TCC GGA GAA CCT GTA TTT TCA GAG CAT GAG CCC GAA AGA CTT GAC GAT ACC GAC CG 3' was used for the forward orientation of the gene, with the BamHI restriction site underlined. The reverse primer was 5' ATT TAA GCG GCC GCT CAA TCG AAA CCC AGC AAC TCG AAA ATT TCG CG 3', with the underlined portion representing the NotI restriction site. The primers included information to encode for a 6x His-tag for purification purposes, as well as a Tev cleavage site for optional removal of the tag upon purification.

After PCR amplification, the gene was inserted into the expression vector by means of restriction digestion using the appropriate restriction enzymes to ensure singularity in direction, then ligation to preserve the integrity of the construct. Upon transformation into chemically competent *E. coli DH5- α* cells, the plasmid was replicated

and harvested using DNA miniprep kit (Qiagen). Gene insertion was confirmed by DNA sequencing (Genewiz). Upon transformation into *E. coli* BL21+ cells, the recombinant protein will dimerize *in vivo* during the induced expression in preparation for purification.

Cloning of DPOR Components – NB-Protein

The cloning strategy for the NB-protein is similar to that of the L-protein, though due to the heterodimeric nature of the protein, certain modifications are taken to ensure appropriate purification products. These measures include the construction of two distinct expression vectors housing either the *BchN* or the *BchB* gene (Figure 2.2). As with the L-protein, the construct for the BchB protein utilizes the RSF-Duet vector, which contains a kanamycin resistance cassette. However, to allow for antibiotic selection, the construct containing the gene encoding for BchN was made using the pET-Duet vector. Rather than kanamycin, the pET vector contains an ampicillin resistance gene. Therefore, each vector is co-transformed and expressed in *E. coli* to ensure proper protein assembly and co-factor incorporation in the cell.

The *BchB* gene was amplified using the forward primer 5' TAA ATT GAG CTC GGA GAA CCT GTA TTT TCA GAG CAT GAA ACT GAC GCT GTG GAC ATA TGA AGG CCC G 3' and the reverse primer 5' GAA GTT GTC GAC TCA CCG TGC ATA ATG AGC TTT CGC CTC GTA C 3'. The underlined restriction sites used in the cloning process are recognized by the SacI in the forward direction, and by SalI in the reverse direction. This expression vector contains an N-terminal 6x His-tag for

purification purposes, with a Tev cleavage sequence immediately downstream for removal of the tag.

The pET vector housing *BchN* was similarly amplified by PCR. The forward primer 5' TAT AAA CAT ATG AGC CTT GAC CTT CCG CCC CCG CCC G 3' includes an NdeI restriction site (underlined portion) which allows for the digestion and insertion into the parent vector. The reverse primer 5'- TAT AAA GGT ACC TCA TTC CGC AGC CTC GCG CCG CAG GAT C -3' incorporates a KpnI restriction site. After PCR amplification, the amplicon was cut using NdeI and KpnI restriction enzymes in preparation for insertion into the pET vector. Unlike the construct for the BchB protein, this construct did not contain a purification tag. When co-expressed with the *BchB* vector, the heterotetramer forms, which allows for the complex to be purified using the 6x His-tag present on the other construct. The recombinant vector was verified by DNA sequencing.

Expression and Cluster Formation of the L-Protein

The expression vector containing the *BchL* gene was transformed into chemically competent BL21+ *E. coli* cells by the addition of 0.5 μL of the purified plasmid into 50 μL of cells. After treatment, the cells were incubated on ice for 20 minutes, after which it was subjected to heat shock at 42°C for 55 seconds, then incubated on ice for an additional 2 minutes. At this point, 250 μL of LB media was added to the transformation, and allowed to incubate at 37°C for 30-45 minutes. The entire volume was plated on LB agar plates containing 50 $\mu\text{g}/\text{mL}$ kanamycin and 0.34 $\mu\text{g}/\text{mL}$ chloramphenicol for appropriate antibiotic selection of cells that have taken up the plasmid during

transformation. The plates were incubated overnight at 37°C to allow for colony formation.

After successful appearance of distinct colonies, 5-50 mL LB broth containing 50 µg/mL kanamycin and 0.34 µg/mL chloramphenicol were inoculated using a single colony from the overnight transformation. This starter culture was allowed to grow overnight at 37°C, after which 1 mL was used to inoculate 1 L LB broth containing 50 µg/mL kanamycin, 0.34 µg/mL chloramphenicol, 1 mM iron (III) citrate, and 1 mM L-cysteine. The antibiotics were included in the growth for plasmid retention, whereas the iron and cysteine served as the source for the iron and sulfur used in the formation of the [4Fe-4S] cluster under anaerobic conditions. The cultures were incubated at 37°C while shaking at 220 rpm initially, as the optical density (O.D.) is monitored by spectrophotometer using the wavelength absorbance at 578 nm. When the O.D. = 0.4, the cultures were shifted from 37°C to 25°C for greater induction control. At O.D. = 0.5, 50 µM isopropyl β-D-1-thiogalactopyranoside (IPTG) is added to each flask to induce the overexpression of the L-protein by regulation of the *lac* operon native to the expression vector. The cultures are allowed to grow at 25°C overnight.

To facilitate proper co-factor insertion for protein function, the remaining steps were carried out under anaerobic, reducing conditions by the addition of 2 mM sodium dithionite. The cultures were transferred to 1L centrifuge bottles where dithionite was added under atmosphere of nitrogen. Each bottle was then incubated at 17°C for three hours prior to centrifugation at 5000 rpm for 20 minutes to collect the cells. While taking care to maintain a nitrogen atmosphere above the reduced cell solution, the cell pellets

were re-suspended in 100 mM HEPES, 10 mM MgCl₂ buffer containing 2 mM dithionite and transferred anaerobically via syringe into sealed vials purged of oxygen and equilibrated with nitrogen. The cells were then frozen and stored at -20°C in preparation for purifying the protein.

Growth and Expression of the NB-Protein

The expression and purification of the NB-protein is virtually identical to that of the L-protein protocol. The expression vectors containing the *BchN* and the *BchB* genes were co-transformed into chemically competent BL21+ *E. coli* cells by the addition of 0.5 µL of each respective plasmid into 50 µL of cells. The transformation was incubated on ice for 20 minutes after the addition of DNA to allow for appropriate incorporation into the cells. Heat shocking at 42°C for 55 seconds allowing for expansion of membrane pores, followed by incubation on ice for an additional 2 minutes ensures successful uptake of foreign DNA. At this point, 250 µL of LB media was added to the transformation, and allowed to incubate at 37°C for 30-45 minutes. The entire volume was plated on LB agar plates containing 50 µg/mL kanamycin, 100 µg/mL ampicillin, and 0.34 µg/mL chloramphenicol. These plates are incubated overnight at 37°C to allow for transformed cell growth.

Following the development of distinct colonies, 5-50 mL LB broth containing 50 µg/mL kanamycin, 100 µg/mL ampicillin, and 0.34 µg/mL chloramphenicol were inoculated using a single colony from the overnight transformation. This starter culture was allowed to grow overnight at 37°C. Following incubation, 1 mL was used to inoculate 1 L LB broth containing 50 µg/mL kanamycin, 100 µg/mL ampicillin, 0.34

$\mu\text{g/mL}$ chloramphenicol, 1 mM iron (III) citrate, and 1 mM L-cysteine. As with the growth for L-protein expression, the antibiotics are included in the growth for plasmid retention, whereas the iron and cysteine serve as the source for the iron and sulfur used in the formation of the [4Fe-4S] cluster under anaerobic conditions. The cultures are placed in incubation at 37°C while shaking at 220 rpm initially, as the optical density (O.D.) is monitored by spectrophotometer using the wavelength absorbance at 578 nm. When the O.D. = 0.4, the cultures are shifted from 37°C to 25°C for greater induction control. At O.D. = 0.5, 50 μM isopropyl β -D-1-thiogalactopyranoside (IPTG) is added to each flask to induce the overexpression of the L-protein by regulation of the *lac* operon native to the expression vector. It is important to strictly follow the O.D. guidelines for expression of NB-protein. Unlike the L-protein, expression of vector which efficiently overexpresses the recombinant protein with proper cofactor incorporation, expression of the NB-protein growth was much more sensitive in general, the result being poorly saturated NB-protein with respect to its metal cluster if these guidelines aren't met. The cultures continue to grow at 25°C overnight for maximum protein production.

To facilitate proper co-factor insertion for protein function, the remaining steps were carried out under anaerobic, reducing conditions by the addition of 2 mM sodium dithionite. The cultures were transferred to 1L centrifuge bottles where dithionite was added under atmosphere of nitrogen. Each bottle was then incubated at 17°C for three hours prior to centrifugation at 5000 rpm for 20 minutes to collect the cells. While taking care to maintain a nitrogen atmosphere above the reduced cell solution, the cell pellets were re-suspended in 100 mM HEPES, 10 mM MgCl_2 buffer containing 2 mM dithionite

and transferred anaerobically via syringe into sealed vials purged of oxygen and equilibrated with nitrogen. The cells are then frozen and stored at -20°C in preparation for purifying the protein.

Purification of DPOR Protein Components

The frozen cells are taken from storage at -20°C and thawed under atmosphere of nitrogen in a room-temperature water bath. At the same time, equilibration buffer containing 100 mM HEPES pH 7.5, and 150 mM NaCl was degassed on a vacuum manifold and replacing the atmosphere with nitrogen. In preparation for column chromatography and lysis methods, the buffer was reduced by addition of 2 mM dithionite. The cells were lysed using a French pressure cell adapted for use to maintain anaerobic conditions. Needles were placed on the in and out lines for transfer and collection into sealed, degassed vials, and a positive atmosphere of nitrogen was maintained above the solutions during the process. To ensure the safety of the protein while in the chamber, 30 mL of reduced equilibration buffer was passed through prior to the addition of the thawed cells. Post lysis, the total cell lysate was transferred anaerobically into centrifuge tubes that have been equilibrated with nitrogen. Centrifugation at 17000 rpm for 1 hour ensures total clarification of the cell lysate into insoluble and soluble fractions. The aqueous portion is transferred carefully into an empty, degassed vial containing 0.7 mL 1 M HEPES pH 7.5, 2.3 mL H_2O , and 350 mg NaCl. Adhering to this step ensures proper charge maintenance on the 6xHis tag for binding to the Ni-NTA column.

This column is made reducing by passing through degassed equilibration buffer containing 2 mM dithionite. Reducing conditions are verified by colorimetric determination using methyl viologen. The protein is then loaded onto the Ni-column, and then rinsed with equilibration buffer. The column is then washed with wash buffer containing 100 mM HEPES pH 7.5, 150 mM NaCl, and 20 mM imidazole. The protein is eluted off of the column using a similar elution buffer that contains 250 mM imidazole. Each buffer is made reducing by the addition of 2 mM dithionite. Protein that is saturated with metal should appear as a dark brown band on the column, which is eluted into a 100 mM HEPES dilution buffer.

The diluted protein is loaded onto a Q-sepharose column which has been pre-washed in a 100% salt solution that has been degassed and reduced with 2 mM dithionite. The protein, again indicated by dark brown coloration is eluted using a NaCl gradient (20%-45%). BchNB will begin elution off of the column at 26% salt, whereas BchL will elute later, at around 35% salt. The protein is eluted into empty, degassed, and sealed vials in preparation for concentration. The proteins are loaded onto a concentrator anaerobically, first using reduced salt buffer to reduce the system, and maintaining nitrogen pressure to protect the purified proteins. Using an appropriate cut-off filter, each protein is concentrated, then stored in liquid nitrogen until needed for use in *in vitro* assays.

Iron content of the purified proteins were analyzed using an iron chelation assay using a α,α' -dipyridal solution. This was accomplished by preparing 5 mM ferrous iron standard solutions containing 0-300 nmol Fe, and treating them with 10 %

hydroxylamine and 20 mM α,α' -dipyridal solution. Known volumes of protein with unknown iron content were analyzed and compared to the standards by reading absorbance at 520 nm. Ratios of iron content/protein were determined by comparing nmol Fe with nmol protein used in the assay, and compared with the theoretical values of 4 Fe/L-protein, and 8 Fe/NB-protein.

Generation and Extraction of Pchl_{ide}

A strain of *Rhodobacter capsulatus* (ZY5) was kindly provided to us by Dr. Carl Bauer (University of Indiana, Bloomington). This strain is deficient of the *BchL* gene, rendering the DPOR complex useless. Thus, growing the strain in dark conditions allows for the accumulation of Pchl_{ide}, which is excreted into the culture medium. First, a 5 mL starter culture is prepared by inoculating RCV-2/3-PY medium containing 5 $\mu\text{g/mL}$ kanamycin from a glycerol stock of cells kept at -80°C . This culture is grown at 34°C while illuminated and slow shaking at 130 rpm. Then a larger volume of culture medium is inoculated from the starter. First, a 125 mL volume is inoculated, followed by a 500 mL growth under the same conditions, with the exception of being grown in the dark for initiation of chlorophyll synthesis. When left overnight, Pchl_{ide} is excreted into the culture medium, without the disruption of cells. The Pchl_{ide} is harvested by centrifugation at 8000 rpm for 30 minutes, followed by filtration through a 0.4 μm filter to remove contaminating cell debris. As the cells remain intact through this procedure, a new culture may be prepared by re-suspending the pellet in fresh RCV-2/3-PY medium. The filtered Pchl_{ide} mixture was placed into a separatory funnel and extracted using one-third volume diethyl ether (Sigma). Due to the rapid expansion of ether, great care is

taken to relieve built up pressure within the funnel by removing the stopper, allowing for the release of vapor. The mixture is shaken to ensure thorough mixing, and the ether phase is separated from the aqueous phase and collected in a clean flask. The viscous inter-phase containing Pchlde is centrifuged at 4300 rpm for 2 minutes to clarify the ether phase, where it is added to the other collected stock. Contamination is removed by cooling on dry ice, and decanted from the solidified water contaminants. The ether phase is evaporated to dryness under a constant nitrogen stream. The dried Pchlde was dissolved in 300 μ L DMSO and stored in a light-sensitive container in the dark. Pchlde concentration is determined by addition into an 80% acetone solution via spectrophotometer, and using the millimolar extinction coefficient of 30.4 at 626 nm.

Pchlde Reduction Endpoint Assay

Pchlde reduction assays were performed to qualitatively observe if the purified DPOR components were capable of the ATP-driven reduction of substrate. Reaction buffer was made which included 50 mM HEPES pH 7.5, 10 mM $MgCl_2$, and 6 mM dithionite. This buffer was purged of oxygen by degassing on a vacuum manifold and replaced the atmosphere with nitrogen. The solution was made reducing afterwards by the addition of 6 mM dithionite, which was degassed separately. Each protein was taken from storage in liquid nitrogen and placed on manifold for degasification. In a separate degassed, empty vial, appropriate volumes of degassed reaction components were added and brought up to 500 μ L final volume using the reduced reaction buffer. The contents were mixed anaerobically using a syringe. A control containing no ATP was made by the addition of 2 μ M NB, 8 μ M L, and 10 μ M Pchlde. The reduction assay contained the

same components, and the reaction was initiated by the addition of 2 mM ATP, mixing with the syringe to homogenize the solution. After ten minutes, the reactions were quenched by the precipitation of proteins by the addition of 800 μL 100% v/v acetone into 200 μL assay mixture. The Pchl_{ide}/Chl_{ide} mixture was harvested by centrifugation at 13000 rpm for ten minutes, at which time the results were obtained by measuring absorbance over a wavelength range of 700 – 580 nm for each condition.

DPOR Steady-state ATPase Kinetics

Steady-state ATPase assays were carried out in anaerobic conditions in sealed, crimp-shut vials. Reaction buffer containing 50 mM HEPES pH 7.5, and 10 mM MgCl₂ was degassed on a vacuum manifold by switching from vacuum to purge oxygen from the system and replacing it with nitrogen gas. Pchl_{ide} and ATP were also degassed in this manner. After degasification, 12 mM dithionite was added to the reaction buffer, which is absent of ATP. Solutions were checked by methyl viologen indicator to see if they were reducing. Empty vials were sealed and degassed to hold all of the reaction components in preparation of starting the assay. BchNB and BchL proteins were taken from storage in liquid nitrogen and degassed prior to addition to vials containing reduced buffer. The amount of protein used in each reaction was 5 μM NB and 20 μM L, along with 20 μM Pchl_{ide}. Each reaction was made up to a final volume of 1 mL with the addition of reduced buffer. To detect ATP hydrolysis, $\alpha\text{-P}^{32}$ -labelled ATP was added to the degassed stock to create a hot ATP mix for use in the assay. Addition of 5 mM ATP was used to start the reaction, which took place at room temperature while mixing periodically by hand. At each time point, 25 μL were taken by syringe and added to 25 μL 0.5 M EDTA

for quenching. Samples were taken from 0-40 minutes. After completion of the assay, the quenched samples from each time point were plotted on a PEI cellulose plate and developed using thin layer chromatography for separation of hydrolyzed ADP from unhydrolyzed ATP. The plates were developed by placement in a chamber containing phosphate buffer pH 3.4 for 70 minutes. Once dried, the plates were placed in a cassette for development for data analysis, and the relative amounts of hydrolysis product determined by pixel quantification.

Preliminary Pre-steady State Analysis of DPOR Activity

Due to the recent findings concerning the pre-steady state dynamics at play in the nitrogenase catalytic mechanism⁸, rapid kinetic techniques were used to characterize events occurring during the first catalytic cycle for DPOR. A combination of radiolabeled ATPase assays using rapid mixing and chemical quench and real-time phosphate release assays were used to obtain first order rate constants for the events of ATP hydrolysis and phosphate release by the L-protein.

Rapid-quench ATPase experiments were carried out using Quench-flow instrumentation by KinTek with 10 μ M NB-protein, 40 μ M L-protein, 40 μ M Pchlide, 1 mM ATP, and 6 mM dithionite in a reaction buffer containing 50 mM HEPES pH 7.5 and 6 mM $MgCl_2$. The reaction buffer was degassed by the use of vacuum manifold hooked up to a vacuum pump to purge oxygen from the system and replace it with a nitrogen atmosphere. The dithionite was added after degasification was complete. To assay for pre-steady state hydrolysis by DPOR, the previously mentioned enzyme components were mixed rapidly with 2 mM ATP and quenched using 0.5 M EDTA. Following

reaction quenching, 1 μ L aliquots were plotted on PEI cellulose thin layer chromatography plates, and developed overnight for computational analysis. The molar amount of ADP formed was plotted versus time to obtain the burst rate of ATP hydrolysis during the pre-steady state.

Real-time kinetic experiments were performed by using a stopped-flow instrument developed by KinTek. ATP hydrolysis and phosphate release from the L-protein was monitored by using a fluorescent probe developed by Dr. Martin Webb⁹ using MDCC-labelled phosphate binding protein (PBP). Change in fluorescence of MDCC-PBP upon phosphate binding was monitored using an excitation wavelength of 435 nm and using an emission cut-off filter of 450 nm. DPOR assays were performed using 0.5 μ M NB-protein, 4 μ M L, 10 μ M Pchlide, and 5 μ M MDCC-PBP in 100 mM HEPES pH 7.5 and 10 mM MgCl₂ buffer. Excess phosphate in the instrument and solutions were scrubbed using a coupled assay containing 200 μ M 7-methyl guanosine and 0.01 U/mL purine nucleoside phosphorylase for 30 minutes prior to data collection. The reaction components were shot against a buffer containing 100 mM HEPES pH 7.5, 10 mM MgCl₂, and 0.5 mM ATP. Upon rapid mixing of the components, the change in fluorescence was monitored in real-time in the observation cell in the instrument.

2.3 RESULTS

Cloning and Expression of DPOR Components from E. coli

The genes *BchL*, *BchN*, and *BchB* were successfully cloned into expression vectors that allowed for overexpression and purification of the L-protein, and the NB-

proteins, respectively. Prior work to isolate DPOR components from *Rhodobacter capsulatus* resulted in total protein yield of close to 4 mg/mL¹. The incorporation of the aforementioned expression vectors proved to be more successful. The transformation and expression of the plasmid containing *BchL* into *E. coli* BL21+ cells yielded close to 100 mg of the purified 64 kDa L-protein homodimer after the two-step purification process over Ni-NTA and Q-sepharose columns (Figure 2.1B). The co-expression of the *BchN* and *BchB* plasmids and subsequent purification methods analogous to those used for the L-protein resulted in similar amounts of purified NB-protein (Figure 2.2B). Iron content analysis by α,α' -dipyridal chelation assays indicate that the purified protein contain roughly 4 Fe atoms/L-protein and 8 Fe atoms/NB-protein, suggesting appropriate [4Fe-4S] cluster formation and incorporation into the DPOR components, even when expressed and purified through an *E. coli* system. Both isolated proteins appear to be > 95 % pure following the purification protocol. Pchlide extracted by use of the ZY5 strain of *Rhodobacter capsulatus* generously provided to us by Dr. Bauer (Bloomington, IN) exhibited absorption maximum at 626 nm as determined in 80% acetone. The concentration of Pchlide, determined by Beer's law is 617 μ M. This successful purification allows for the initial characterization of the ability of DPOR to reduce Pchlide, and how the hydrolysis of ATP helps to accomplish that goal.

Steady-state ATPase Analysis and Pchlide Reduction of DPOR

After isolating the purified DPOR complex, the next step was to assay for the capability to reduce Pchlide within the NB-protein coupled to the hydrolysis of ATP by the L-protein. The purified protein complex was capable of reducing Pchlide to Chlide as

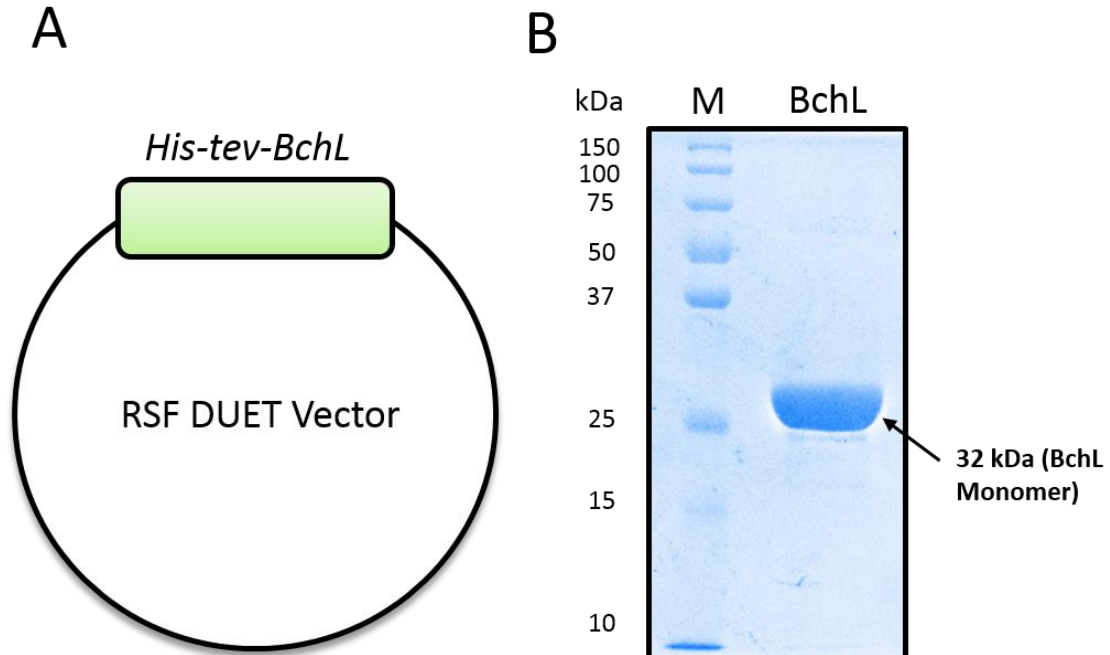


Figure 2.1. Strategy and Purification of BchL. (A) Genetic construction of the BchL containing vector. The gene encoding for the BchL protein was successfully cloned into an RSF-duet expression vector and transformed into *E. coli* BL21+ cells. (B) Expression and purification of BchL. The addition of isopropyl β -D-1-thiogalactopyranoside (IPTG) triggers the production of BchL by stimulation of the lac operon. Once expressed, the protein was able to incorporate the [4Fe-4S] cluster necessary for catalysis using iron (III) citrate and L-cysteine supplemented in the culture medium. The L-protein was able to be successfully isolated anaerobically using a two-step chromatographic approach by passing the cell lysate over Ni and anion-exchange columns. The resulting protein isolate is >95% pure, evidenced by SDS-PAGE.

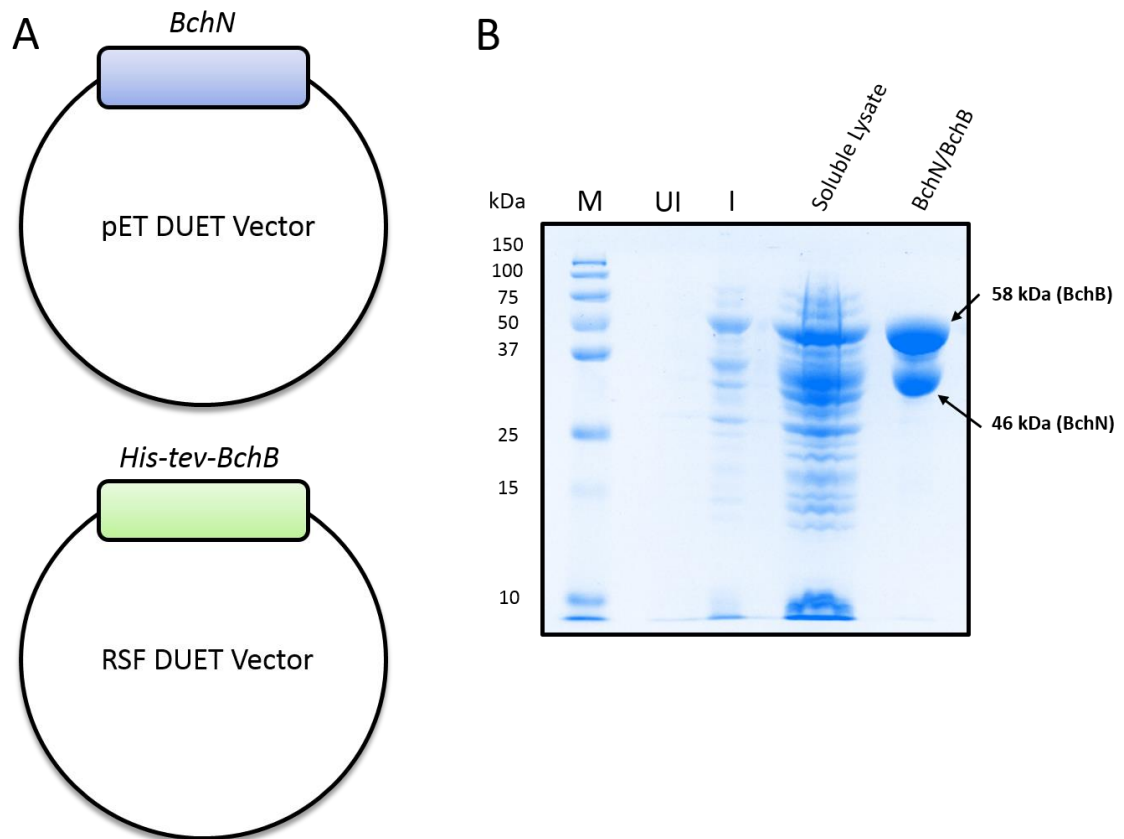


Figure 2.2. Cloning strategy and Purification of the BchNB protein. (A) Vector components of BchNB. The strategy for isolating the NB-protein of the DPOR complex involves the dual transformation and expression of the BchN protein in the pET-Duet vector, and the BchB protein in the RSF-Duet vector using the *E. coli* BL21+ expression system. (B). Expression and purification of BchNB. These constructs were able to be expressed sufficiently under IPTG induction, with metal clusters appropriately formed and incorporated when introduced to anaerobic conditions by the addition of 2 mM dithionite. The two-step purification process of Ni-affinity chromatography and anion-exchange chromatography was successful in isolating the functional protein to greater than 95% purity.

indicated by a spectral shift from 626 nm to 665 nm (Figure 2.3). This assay was accomplished under anaerobic conditions with 2 μ M NB-protein, 8 μ M L-protein, 10 μ M Pchl_a, and were initiated by the addition of 2 mM ATP. DPOR exhibits significant Pchl_a reduction as evidenced by the appearance of Chl_a after 5 min. Because of this successful transformation from substrate into product, Steady state ATPase kinetic assays were performed to observe and probe the ATP requirement of the reaction.

The assays performed with conditions stated above successfully allowed for the observation of how quickly DPOR is able to turnover ATP as an obligate step in the reaction mechanism during the steady state. Until now, these findings remained largely unanswered. DPOR is capable of turning over ATP at a slow steady-state rate of 4.07 μ M ATP hydrolyzed per minute as evidenced by PEI sepharose thin layer chromatography (Figure 2.4A). Adjusting for the stoichiometric ratio of μ M ATP hydrolyzed/NB-protein, the k_{cat} was found to be 0.0135 second^{-1} (Figure 2.4B). Interestingly, this rate for ATP hydrolysis is found to be roughly 400 fold slower than the observed k_{cat} for the nitrogenase ATP hydrolysis by the Fe protein, which was found to be 5.6 second^{-1} . Considering the difficulty of reduction of the nitrogen-nitrogen triple bond, and the number of single electron transfer cycles required by nitrogenase (8 as opposed to 2), this begs the question of why the ATPase cycle occurs much slower in the steady state.

Pre-steady state Analysis of the L-Protein Catalyzed ATPase Cycle

The discrepancy between the steady-state activity between nitrogenase and DPOR was so apparent, that a deeper probe into the catalytic mechanism became necessary in order to explain why nitrogenase is a more robust ATP utilizing engine. From recent

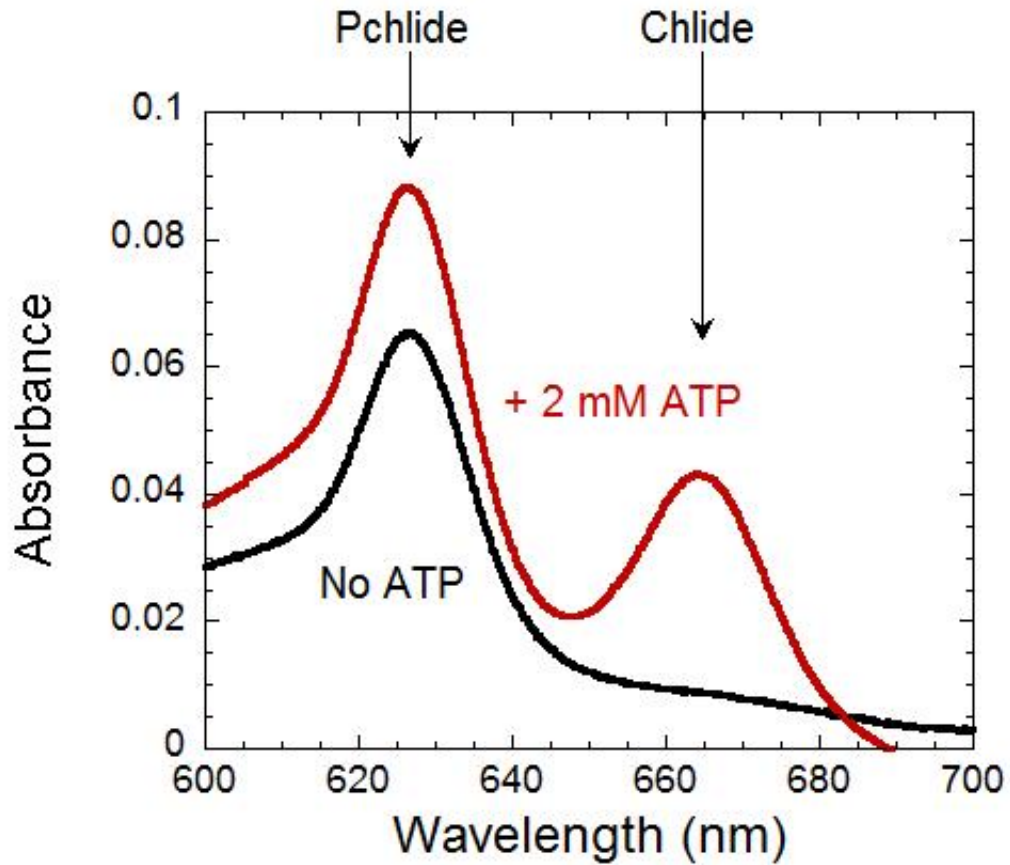


Figure 2.3. Pchl a₂ reduction assay using isolated DPOR components. The purified BchL and BchNB proteins were used for the initial *in vitro* characterization of activity by incubation of 10 μ M Pchl a₂ with 2 μ M NB-protein and 8 μ M L-protein at room temperature. After the addition of 2 mM ATP, significant Chl a₂ formation is observed after 5 minutes. In the condition where the DPOR components were incubated in the absence of ATP, no substrate reduction was monitored.

studies into the nitrogenase pre-steady state single-electron transfer cycle⁸, it is known that electron transfer occurs quickly ($k_{ET} = 140 \text{ second}^{-1}$) and precedes the step of ATP hydrolysis, which occurs at $k_{ATP} = 70 \text{ second}^{-1}$.

Similar rapid kinetic approaches listed above (rapid mixing chemical quench assays and real-time phosphate release assays) allowed for the observation of the principle steps of ATP hydrolysis and P_i release, which illuminated the rates at which these steps occur in the catalytic mechanism. Using the reconstituted DPOR complex, mixed with $\alpha\text{-P}^{32}$ -labelled ATP for varying times allowed for the ability to observe the pre-steady state ATPase activity (Figure 2.5A). Interestingly, only two of the four bound ATP of the DPOR complex were hydrolyzed in the pre-steady state, and this hydrolysis occurs rapidly, with a $k_{ATP} = 73 \text{ second}^{-1}$, which closely mirrors that which is observed in the nitrogenase pre-steady state. These data also suggest that the initial hydrolysis of the two ATP occurs at a rate that is roughly 900 times faster than the steady state rate of ATP hydrolysis, and therefore, cannot be the rate-limiting step in the reaction. To probe ATP catalysis further, P_i release experiments were performed in real-time by use of an MDCC-labelled phosphate binding protein probe⁹ developed for the purpose of rapid kinetic assays. When DPOR reaction mixture containing MDCC-PBP was mixed rapidly with ATP, the change in fluorescence was monitored, and found to be much slower than the rate of initial ATP hydrolysis ($k_{P_i} = 0.07 \text{ second}^{-1}$) (Figure 2.5B). These data suggest that phosphate release, while much slower than the initial rate of ATP hydrolysis in the pre-steady state, does not constitute the rate-limiting step in the process, and that the slow

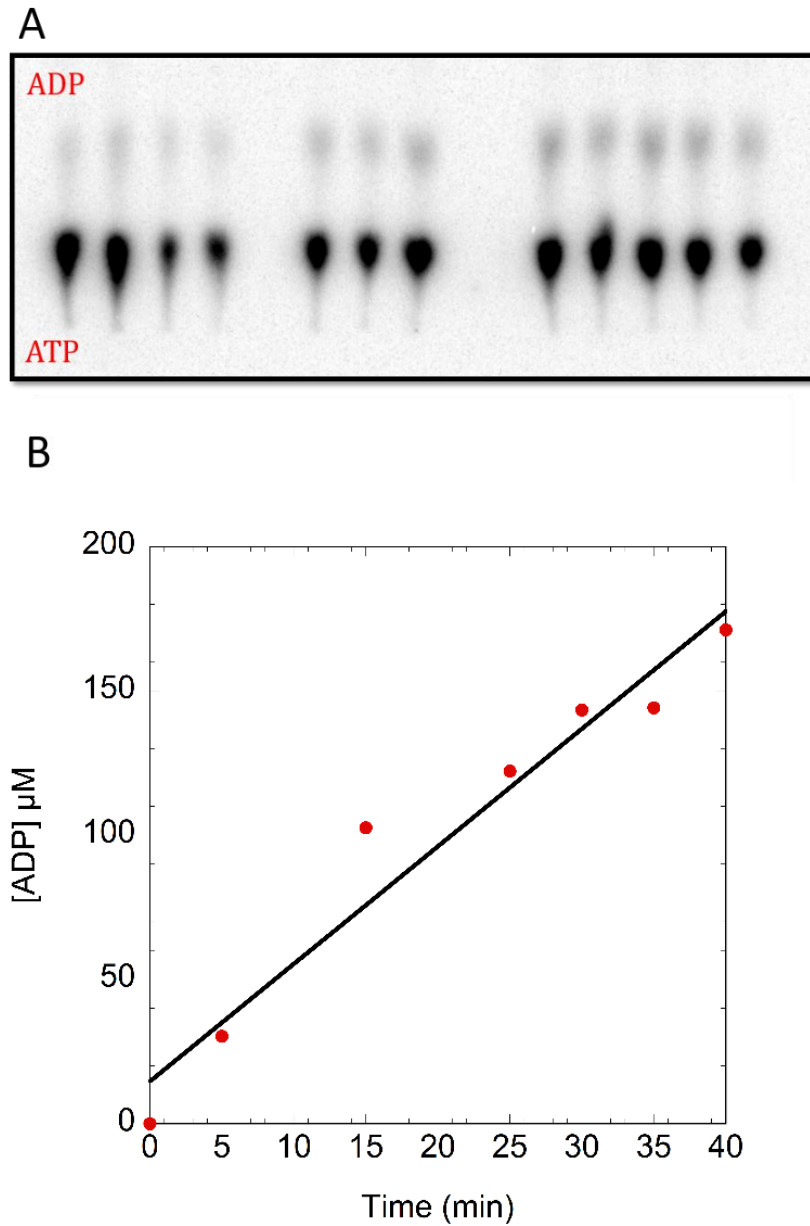


Figure 2.4. Steady-state analysis of DPOR ATPase activity. (A) PEI-cellulose thin-layer chromatography results. DPOR was assayed for ATPase activity using α - P^{32} -labelled ATP incubated with 5 μ M NB-protein, 20 μ M L-protein, and 20 μ M Pchl_d and quenching using 0.5 M EDTA pH 8.0. 1 μ L volume from each time point was plotted on a PEI-cellulose plate for analysis. (B) Steady state ATPase Kinetics. After imaging the thin-layer chromatography results, the amount of ATP hydrolysis was quantified and plotted versus time. ATP is hydrolyzed slowly with a $k_{cat} = 0.0135 \text{ second}^{-1}$.

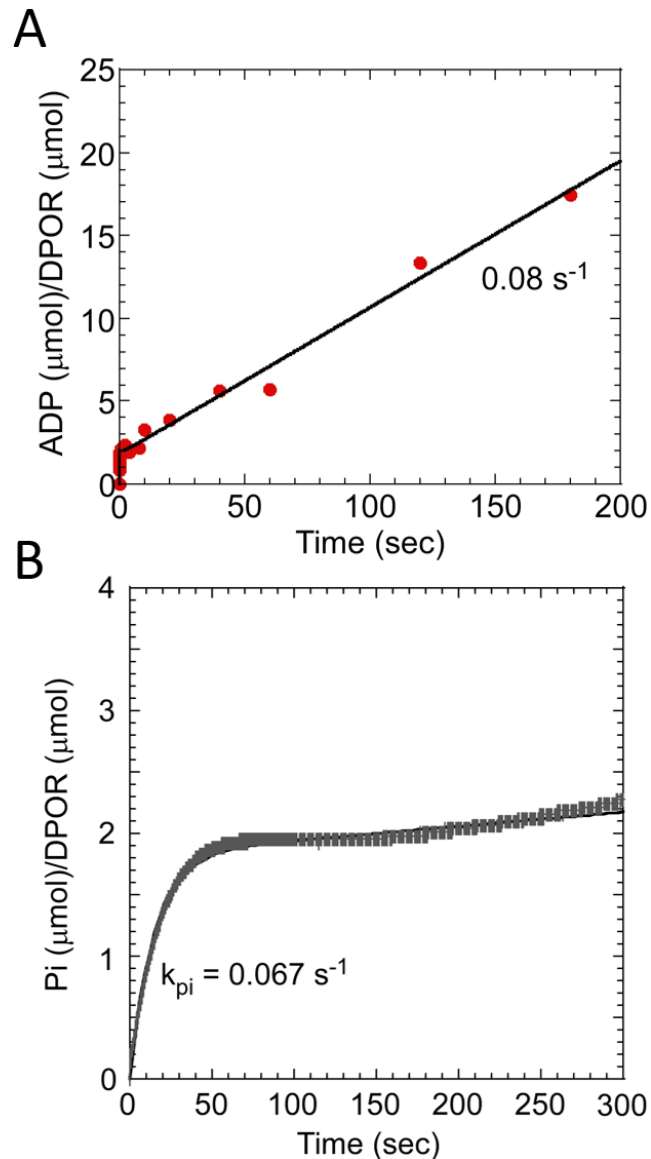


Figure 2.5. Pre-steady state kinetic characterization of DPOR. (A) Quench-flow ATPase assay. Pre-steady state ATPase activity was monitored by incubating $10 \mu\text{M}$ NB-protein, $40 \mu\text{M}$ L-protein, and $40 \mu\text{M}$ Pchl_{ide}, which is rapidly mixed with solution containing 2 mM ATP to initiate the reaction followed by chemical quenching using 0.5 M EDTA pH 8.0 at each time point. While the steady-state rate for ATP hydrolysis is slow, the k_{cat} in the burst phase of catalysis closely resembles nitrogenase kinetics, registering a $k_{\text{cat}} = 73 \text{ second}^{-1}$. (B) Phosphate release studies. Phosphate product release was monitored using a fluorescent probe provided by Dr. Martin Webb. Using stopped-flow kinetic analysis, the rate constant for phosphate release was determined to be $0.067 \text{ second}^{-1}$.

step must occur shortly afterwards, with the two most likely candidates being the release of ADP, or the dissociation of the L-protein from the DPOR complex.

2.4 DISCUSSION

DPOR is an essential enzyme in photosynthetic organisms that catalyzes the reaction which serves as the penultimate step in chlorophyll biosynthesis—the two electron reduction of Pchl_{id} to Chl_{id}. This step is significant in the synthetic pathway because it represents the immediate step prior to the genesis of active chlorophyll for use in photosynthesis, and also serves as the rate-limiting step with respect to its kinetics. While other lab groups have succeeded in characterizing the ability of DPOR to facilitate Pchl_{id} reduction, the characterization of DPOR with respect to its single-electron transfer cycle, as catalyzed by the L-protein, has remained largely mysterious. Only recently has this cycle been kinetically characterized in the nitrogenase system⁸. To address how DPOR uses the energy from ATP to facilitate substrate reduction, and to provide evidence for the molecular basis for allosteric cross-talk between subunits located 98 Å apart, we were able to isolate each protein component, and use *in vitro* rapid kinetic and steady-state assays to monitor ATP hydrolysis at all steps of the catalytic cycle. These resulting data provide intriguing insights into the single-electron L-protein cycle which functions during substrate reduction.

We were successful in the construction of plasmids containing the *BchL*, *BchN*, and *BchB* genes. The introduction of these plasmids into BL21+ *E. coli* cells allowed for the over-expression of both the L-protein, and the NB-protein. These protein components were able to be purified using a two-step method involving Ni-NTA and Q-sepharose

column chromatography methods. The high resulting yield (over 100 mg) allowed for the ability to easily collect large amounts of purified complex for experiments that require high concentrations of protein for detection of signal, such as EPR, and the previously described pre-steady state ATPase experiments. The isolated protein is both occupied with metal, consistent with the levels of iron chelation from α, α' -dipyridal assays, and exhibits ATP-dependent reduction of Pchlide to Chlide, as indicated by a spectral shift of absorbance maximum from 626 nm to 665 nm. Significant transformation of substrate to product is observed after five minutes upon the addition of ATP, which suggests that sufficient levels of Chlide are manufactured within this time frame to be observed by spectrophotometer. Even though the steady-state reaction rate is slow, especially with respect to nitrogenase, the observation of key events should agree with this time frame. Therefore, the isolation of the DPOR complex, and the initial characterization of its activity provide credence to the subsequent kinetic characterization with respect to its ability to hydrolyze ATP.

ATP Hydrolysis Occurs Slowly in the Steady-state

Even though substrate is capable of being reduced to product within the first five minutes of reaction initiation, it was found that DPOR is only capable of hydrolyzing ATP very slowly, as was observed during the steady-state kinetics assay using α - P^{32} -labelled ATP. The rate constant for the steady state hydrolysis occurs at $k_{ATP} = 0.0135 \text{ second}^{-1}$. When compared to the steady state of nitrogenase catalyzed ATP hydrolysis by the Fe-protein, it was found that DPOR is 400 times slower in the steady state. A number of reasons may contribute to this phenomenon. For instance, when the structure was first

determined for the L-protein⁶, the nucleotide-dependent rates of iron cluster chelation by an α,α' -dipyridal compound were found to be much slower. This may suggest a difference in L-protein dynamics that are not seen in the Fe-protein upon binding of nucleotide, which positions the [4Fe-4S] cluster in a position to deliver a single electron before ATP is hydrolyzed.

Additionally, nitrogenase functions by storing accumulated negative charge delivered in single-electron transfer cycles on the face of the FeMo cofactor in the MoFe protein as metal hydrides. When sufficient charge has been accumulated, the triple bond of nitrogen is broken, and subsequently reduced to form two equivalents of ammonia. DPOR differs in that there is no metal cluster at the site of Pchlide binding. Rather, electrons are delivered, one at a time, from the L-protein to the NB cluster, which are used to form an anionic substrate radical, followed by a neutral radical, and finally to a carbanion intermediate before the final proton addition resolves the charge and completes the trans-specific reduction of the Pchlide C17=C18 double bond, forming Chlide as the product. Because of the relative instability of the key reaction intermediates that are formed on the substrate during the catalytic mechanism, it is likely that the rate is affected as a result.

Preliminary Pre-steady State Data Suggest Rapid-burst ATP Hydrolysis on One Half of the DPOR Complex

With the revelation that the steady-state hydrolysis of ATP occurs very slowly, pre-steady state kinetic techniques were used in order to gain mechanistic clues to what the slow step of the DPOR reaction may be. In nitrogenase, the slow step of the reaction

was found to be the dissociation of the Fe-protein from the complex after electron transfer and ATP hydrolysis and product release occur⁸. The rapid-kinetic chemical quench experiments using radiolabeled ATP show promising preliminary data that help describe similarities to the nitrogenase single-electron cycle. Interestingly, there is an initial burst rate for ATP hydrolysis that was found to occur with a first-order rate constant of $k_{\text{ATP}} = 73 \text{ second}^{-1}$. When compared to the steady-state rate, this represents a difference of close to 900 fold, indicating that even though the overall steady-state rate of hydrolysis is much slower, ATP hydrolysis is not rate limiting in the kinetic mechanism. This indicates that the slow step in the catalytic mechanism must occur later on in the catalytic cycle. Additionally, the data suggest that a stoichiometric value of two ATP molecules are hydrolyzed per equivalent of DPOR complex. This could be interpreted in a couple of different ways—either one ATP is hydrolyzed on each side of the DPOR complex simultaneously, or the two ATP bound on one L-protein on one half of the functional complex are hydrolyzed first. The latter would suggest an asymmetric model for ATP utilization by DPOR, which is only strengthened when considering the subunit cross-talk that is inferred when considering the structure for the NB-protein¹⁰ and the evidence based on data from the Pchlide intermediate species during catalysis³. DPOR was shown to form substrate radicals as a function of single-electron transfer by the L-protein, followed by the addition of one proton to relieve charge. During the catalytic cycle, one of the necessary proton donors is thought to come from residue Asp274, which is located on the BchB protein that is not bound to the Pchlide which is being reduced. While further characterization is required, these data indicate a potential sequential mechanism of substrate reduction and ATP hydrolysis, in which catalytic events

occurring on one catalytic half cooperatively trigger queues for the other catalytic half to initiate appropriate chemistry, much like what is observed in a two-cylinder engine.

With the observation of burst kinetics with respect to ATP hydrolysis, it became necessary to address the question of why catalysis by DPOR occurs so slowly in the steady state. The real-time phosphate release data provides insight into what happens after hydrolysis of ATP occurs. Since P_i scavenging by MDCC-PBP occurs rapidly ($k_{\text{on}} = 1.36 \times 10^8 \text{ M}^{-1} \text{ second}^{-1}$) and with high affinity ($K_d = 100 \text{ nM}$) the observed change in fluorescence may be directly correlated to the immediate, diffusion-limited release of P_i from DPOR following ATP hydrolysis. At this point in the kinetic mechanism, the rate-constant of P_i release is found to be much slower than the rate constant for burst ATP hydrolysis ($k_{\text{ATP}} = 73 \text{ second}^{-1}$ versus $k_{P_i} = 0.067 \text{ second}^{-1}$). Since the steady-state rate for DPOR catalysis is still slower than the observed rate for P_i release, the slow step in the catalytic mechanism must occur at some point after this step. In nitrogenase, the slow step was determined to be the dissociation of Fe-protein from the MoFe protein⁸ ($k_{\text{diss}} = 6 \text{ second}^{-1}$). Because of the similarities between the two enzymatic systems, the slow step in DPOR catalysis could very well be the dissociation of L-protein from NB-protein, though the single-electron reduction of Pchlide leading to the formation of substrate radicals could also contribute to the kinetic slow step. The dynamics at play involving ATP during the DPOR reaction mechanism play an interesting role in substrate reduction. However, to further probe mechanistically on how the energy from hydrolysis of ATP is used to accomplish the transformation of Pchlide into Chlide, mutational studies on the L-protein must be achieved that affect ATP binding and hydrolysis. Chapter III describes

the dynamics of the L-protein and discusses the nature and rationale of these mutations, as well as addresses their effect on substrate reduction.

REFERENCES

1. Nomata, J., Swem, L. R., Bauer, C. E., Fujita, Y. Overexpression and characterization of dark-operative protochlorophyllide reductase from *Rhodobacter capsulatus*. *Biochim Biophys Acta* **1708** (2), 229-37 (2005).
2. Nomata, J., Ogawa, T., Kitashima, M., Inoue, K., Fujita, Y. NB-protein (BchN-BchB) of dark-operative protochlorophyllide reductase is the catalytic component containing oxygen-tolerant Fe-S clusters. *FEBS Lett* **582** (9), 1346-50 (2008).
3. Nomata, J., Kondo, T., Mizoguchi, T., Tamiaki, H., Itoh, S., Fujita, Y. Dark-operative protochlorophyllide oxidoreductase generates substrate radicals by an iron-sulphur cluster in bacteriochlorophyll biosynthesis. *Sci Rep* **4**, 5455 (2014).
4. Brocker, M. J., Virus, S., Ganskow, S., Heathcote, P., Heinz, D. W., Schubert, W. D., Jahn, D., Moser, J. ATP-driven reduction by dark-operative protochlorophyllide oxidoreductase from *Chlorobium tepidum* mechanistically resembles nitrogenase catalysis. *J Biol Chem* **283** (16), 10559-67 (2008).
5. Yamamoto, H., Kurumiya, S., Ohashi, R., Fujita, Y. Oxygen sensitivity of a nitrogenase-like protochlorophyllide reductase from the cyanobacterium *Leptolyngbya boryana*. *Plant Cell Physiol* **50** (9), 1663-73 (2009).
6. Sarma, R., Barney, B. M., Hamilton, T. L., Jones, A., Seefeldt, L. C., Peters, J. W. Crystal structure of the L protein of *Rhodobacter sphaeroides* light-independent protochlorophyllide reductase with MgADP bound: a homologue of the nitrogenase Fe protein. *Biochemistry* **47** (49), 13004-15 (2008).
7. Moser, J., Brocker, M. J. Methods for nitrogenase-like dark operative protochlorophyllide oxidoreductase. *Methods Mol Biol* **766**, 129-43 (2011).
8. Duval, S., Danyal, K., Shaw, S., Lytle, A. K., Dean, D. R., Hoffman, B. M., Antony, E., Seefeldt, L. C. Electron transfer precedes ATP hydrolysis during nitrogenase catalysis. *Proc Natl Acad Sci U S A* **110** (41), 16414-9 (2013).
9. Hirshberg, M., Henrick, K., Haire, L. L., Vasisht, N., Brune, M., Corrie, J. E., Webb, M. R. Crystal structure of phosphate binding protein labeled with a coumarin fluorophore, a probe for inorganic phosphate. *Biochemistry* **37** (29), 10381-5 (1998).
10. Muraki, N., Nomata, J., Ebata, K., Mizoguchi, T., Shiba, T., Tamiaki, H., Kurisu, G., Fujita, Y. X-ray crystal structure of the light-independent protochlorophyllide reductase. *Nature* **465** (7294), 110-4 (2010).

CHAPTER III

CONSTRUCTION OF LINKED L-PROTEIN CONSTRUCTS TO INVESTIGATE ATP-RELATED DYNAMICS

3.1 INTRODUCTION

Pchlide reduction as mediated by DPOR involves, by necessity, carefully controlled ATPase activity which is critical for catalysis. Interestingly, the number of events including electron transfer, ATP hydrolysis, and L-protein dissociation are carefully coordinated between symmetrical catalytic halves in what seems to give evidence of allosteric cross-talk. Similarly, these events correlate strongly to what is observed in the nitrogenase system, with the exception that catalysis occurs much more slowly after the initial electron-transferring and ATP hydrolyzing events (Chapter II). The overall subunit architecture and proposed catalytic mechanism highlight a truly dynamic process with a high degree of communication required to achieve substrate reduction. While the first-order rate constants for these steps have been established previously in Chapter II to propose a catalytic order-of-events, that information alone does not address the complexity and communication that occurs as Pchlide is reduced to Chlide, particularly during the binding and hydrolysis of ATP.

In order to gain better understanding on how the ATPase activity of the L-protein helps to facilitate activity in the catalytic NB-protein, a look into nitrogenase Fe-protein mechanics are warranted. During catalysis, as the Fe-protein mediates ATP hydrolysis,

distinct conformations are adopted depending on the state in which the nucleotide is situated^{1,2}. Researchers found that the Fe-protein docks onto the MoFe-protein at a specific surface interface when no nucleotide is bound. Alternate conformations are adopted when ATP is bound to the Fe-protein, then during catalysis, a different conformation is accepted with ADP bound. In all, from the beginning of Fe-protein interaction with the MoFe-protein, the conformation is shifted by about 20° as the nucleotide undergoes hydrolysis. This seems to imply a rolling motion of the Fe-protein as it interacts with the MoFe-protein throughout the catalytic cycle.

The ATP-related dynamics of the Fe-protein are additionally highlighted by mutational studies involving key residues involved in the binding of nucleotide³, as well as with post-hydrolysis signal transduction⁴. Upon binding of nucleotide, the Fe-protein undergoes conformational changes that alter the properties of the [4Fe-4S] cluster, in that the redox potential is reduced from -290 mV to -420 mV, which seems to correlate to an ability to transfer an electron to the awaiting MoFe-protein⁵. It turns out that the binding of nucleotide to the protein involves a shift in the protein chain from Asp 125 to Cys 132, which directly bridges the ATP-binding site and the metal cluster. Shortening this chain by one amino acid at residue Leu 127 created a state which mimicked the ATP-bound protein, including a lower redox potential of its cluster, even though no nucleotide is present.

Additional mutational studies reveal critical information related to ATP binding in preparation for catalysis. In general, ATP motors contain similar structural motifs that mediate crucial interactions between the protein and incoming nucleotide, which serve to

stabilize the transition state during hydrolysis². These motifs have been characterized and are referred to as P-loops, or Walker A motifs, the characteristic sequence reading as follows: GXXXXGKS/T. The lysine embedded within this sequence is especially important for mediating the interaction between the γ -phosphate of the incoming molecule of ATP and the protein prior to catalysis. Nitrogenase, along with DPOR, contains a conserved lysine residue near the N-terminus of the protein. In the case of nitrogenase (*Azotobacter vinelandii* numbering) Lys 15 is the residue in question, whereas Lys 44 is the numbering for the L-protein from *Rhodobacter sphaeroides* (Figure 3.1). In the case of nitrogenase, when the Walker A lysine residue is converted into a different amino acid, such as glutamine, there is a marked decrease in ATP binding when compared to wild-type values, in addition to a total loss of activity, with respect to acetylene reduction, dihydrogen evolution, and ATP hydrolysis³. Due to the high degree of similarity between the Fe-protein and the L-protein in DPOR, it is assumed that a similar mutation to the Walker A lysine residue will yield a mutant that is unable to produce Chlide.

There are, however, additional questions that are worth noting. As the L-protein is a homodimer comprised of identical subunits, the introduction of a point mutation will be seen on both monomeric polypeptide chains, resulting in a protein that is incapable of binding ATP across both nucleotide interaction sites. Thus, would the introduction of only one point mutation, leaving one ATP site intact produce a phenotype that is still capable of Pchlide reduction, and does each ATP have a distinct role during catalysis? Is it possible that the hydrolysis of each individual molecule of ATP contributes to the

rolling motion of the Fe-protein during its interaction with the MoFe protein, and do the proposed dynamics function in DPOR? The answers to these questions have not yet been addressed in the literature to date, and the following studies hope to give insight into

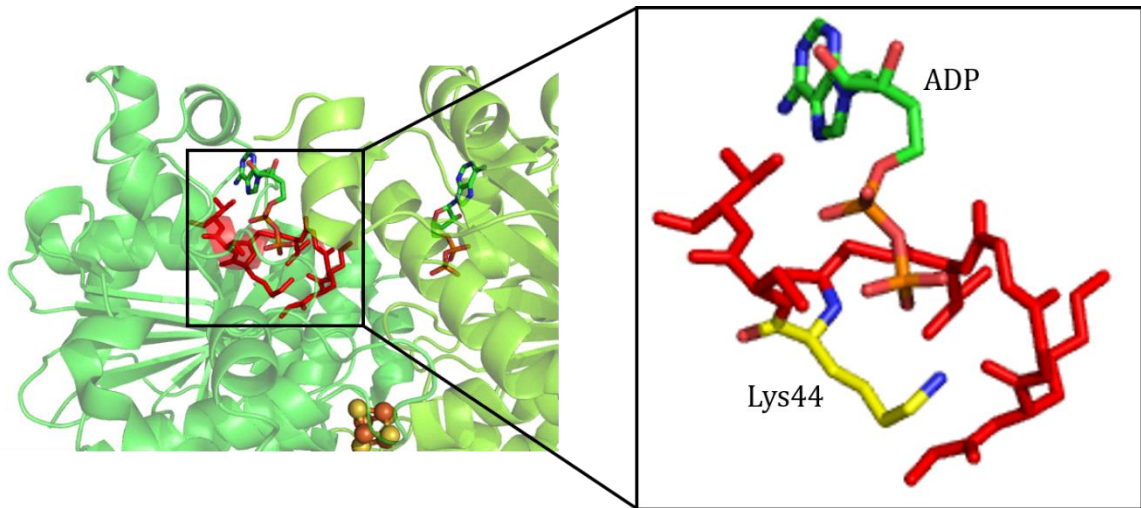


Figure 3.1. Walker A motif in BchL from *Rhodobacter sphaeroides*. BchL, as with other ATPase motors contains conserved sequences that are essential for ATP binding and hydrolysis. The Walker A motif (red) is highlighted to show the proximity it has towards the incoming nucleotide in the binding pocket. Lysine 44 (yellow) provides an essential charge stabilization with the γ -phosphate of the incoming molecule of ATP that also serves to stabilize the transition state during hydrolysis. Studies in nitrogenase show that the mutation of the Walker A lysine residue results in a protein incapable of substrate reduction, but is capable of binding the ADP form.

these queries by developing novel heterodimeric L-protein constructs to investigate the role of each individual ATPase site (Figure 3.2). The constructs generated include the wild-type L-protein to illustrate normal DPOR function, a homodimeric linked L-protein construct incorporating a 3x glycine linker flanked by two *tev* protease cleavage sequences to aid in the removal of the linker post-translationally, and post-purification, a homodimeric L-protein in which both Walker A lysine residues have been mutated to

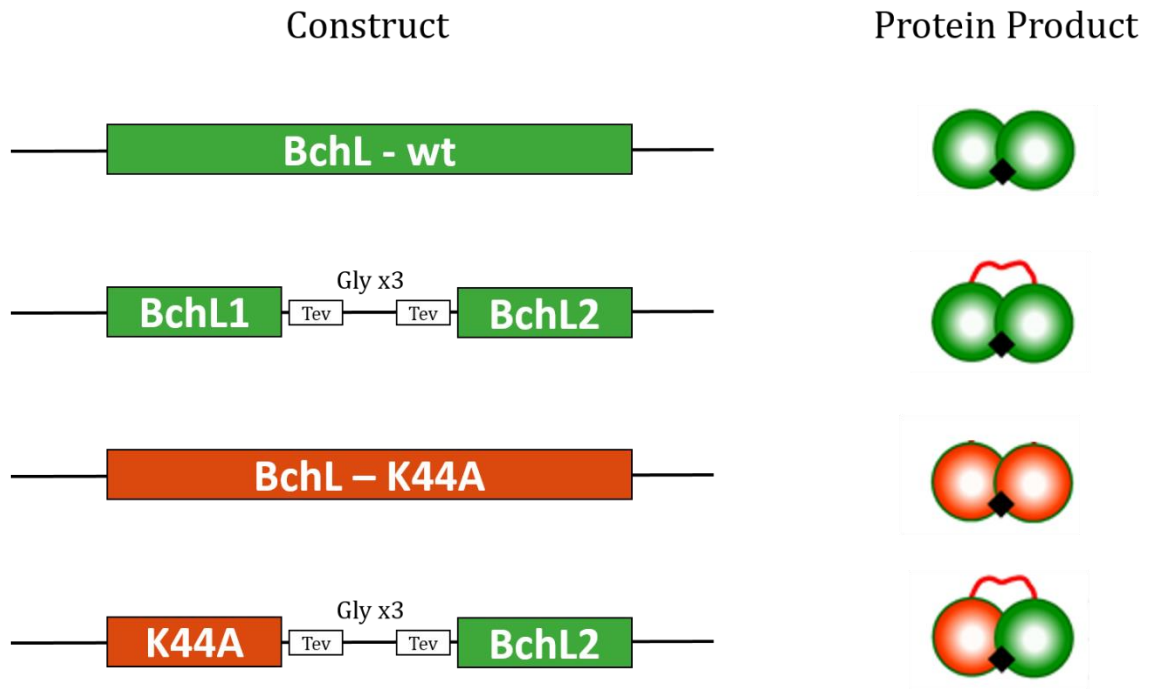


Figure 3.2. List of L-protein constructs and their protein architecture. For the purposes of studying dynamics that occur during DPOR catalysis, an assortment of L-protein variants were designed which may have normal ATPase activity (green) or impaired activity due to the mutation of Lys44 of the Walker A motif to an alanine (K44A) (red).

alanine residues (K44A), and a heterodimeric linked L-protein construct in which one ATPase site has been left intact, while the other site has undergone a point mutation at the Walker A lysine at position 44. We were able to successfully generate each mutant by using standard molecular biology techniques first to generate the homodimeric linked L-protein construct, and then to use strategic site-directed mutagenesis, followed by restriction enzyme digestion/ligation to form the heterodimeric linked L-protein in which one ATPase site has been rendered inert. Each of the constructs were successfully

introduced into an *E. coli* expression system and isolated using affinity chromatography. The homodimeric linked L-protein construct when added to NB-protein, Pchl_{ide}, and Mg-ATP in vitro exhibits activity that is reminiscent of what is observed in the wild-type system with respect to Pchl_{ide} reduction. As expected, the homodimeric Walker A mutant did not show any Chl_{ide} formation, even after 30 minutes. Likewise, the heterodimeric Walker A mutant showed similar inactivity. Suggesting that both ATPase sites are essential for proper function. This chapter details the construction of each novel construct produced, and their insight into the dynamics required for normal DPOR catalysis and Pchl_{ide} reduction.

3.2 METHODS

Plasmid Construction of the Homodimeric Linked L-protein

The construct described in Chapter II which encodes the L-protein from *Rhodobacter sphaeroides* was used as a template for the creation of a vector which will yield a homodimeric linked L-protein in a single polypeptide chain upon gene expression mediated by IPTG induction. Our construct features the aforementioned *BchL* gene in an RSF-duet parent vector, which was used as a template to create each copy of the gene, designated L₁ and L₂, respectively. The gene which would encode for the L₁ monomer was created first using PCR using the reverse primer with sequence 5' ATT ATT CAT ATG GTC GAC TGA TTG GAA GTA TAG ATT CTC TGC GGC CGC TCC ATC GAA ACC CAG CAA CTC GAA AAT TTC GCG ATC CGG CAG CG 3', and the ACYC duet-up1 forward primer, which is specific for the RSF-duet vector. The reverse primer was designed to eliminate the stop codon at the end of the *BchL* gene to ensure

proper read-through of the linked construct during translation, includes a *tev* protease recognition sequence for post-translational removal of the linking unit between both monomeric units, and an NdeI restriction site for cloning purposes. After PCR amplification, the product was digested using BamHI and NdeI restriction enzymes, and placed into an empty RSF-duet vector and ligated using DNA ligase. The ligated product was then transformed into chemically competent DH5- α cells for plasmid replication and harvesting by DNA miniprep (Qiagen). The correct inclusion of the aforementioned features was verified by DNA sequencing (Genewiz).

The L₂ portion of the linked homodimer was similarly constructed, again using the original RSF-duet vector containing the wild-type *BchL* gene as a template. A second PCR reaction was performed, this time using an L₂ specific forward primer with the following sequence: 5' AAT AAT CAT ATG GAG AAT CTA TAC TTC CAA TCA AAG CTT ATG AGC CCG AAA GAC TTG ACG ATA CCG ACC GGA GCG GAT GGC GAG GGC TCG GTC CAG GTG C 3'. This primer contains information for the other half of the linker between the L₁ and L₂ genes, as well as a second *tev* protease recognition sequence. The use of dual *tev* sites ensures that upon incubation of the translated homodimeric linked protein with protease, that the majority of the linker will be completely removed, without leaving overly long segments which may contribute to non-native secondary structure elements. Like with the above construct, the product was digested with the restriction enzymes NdeI and KpnI prior to incubation with a similarly cut RSF-duet vector and inserted by incubation with DNA ligase. The freshly-ligated

DNA was then transformed into chemically competent DH5- α cells for mass replication and harvesting, as previously described.

With the successful construction of both the L₁ and L₂ constructs in the RSF-duet vector verified by DNA sequencing, the construction of the homodimeric L₁-L₂ linked construct became possible. To accomplish this, the construct containing the L₂ gene in RSF duet was digested with the NdeI and BamHI restriction enzymes in preparation of receiving the L₁ segment. This was prepared by the digestion of the L₁-containing RSF-duet vector using the same restriction enzymes mentioned previously, and verifying appropriate insert size by TBE-agarose gel electrophoresis. Upon verification of appropriate vector digestion, the insert was selectively purified from the gel using a DNA gel extraction kit (Qiagen), and incubated with the L₂-containing digested vector. The resulting ligated vector was transformed into DH5- α cells, again for mass-production of the L₁-L₂ linked construct in RSF-duet. Similar to the un-linked, wild-type construct, the vector contains information encoding for an N-terminal 6x His-tag to aid in affinity purification over a Ni-NTA column.

Site-directed Mutagenesis and Construction of the K44A Walker A Mutant L-Proteins

Site-directed mutagenesis of the wild-type L-protein was used to generate a novel mutant construct in which both ATPase subunits were rendered inactive with respect to nucleotide binding by the point mutation of Lys44 (*Rhodobacter sphaeroides* numbering) to an alanine (K44A). The RSF-duet vector containing the wild-type *BchL* gene was used as a template in a mutagenesis reaction performed in a thermocycler using the QuikChange II XL Site-Directed Mutagenesis Kit (Agilent Technologies) with the

forward primer 5' CGA GGT CGT CGA CGC GCC GAT CCC GCC C 3', and the reverse primer 5' GGG CGG GAT CGG CGC GTC GAC GAC CTC G 3'. The underlined segments denote the mismatches necessary for the mutagenesis to occur. After the polymerization reaction was completed, the restriction enzyme DpnI was added for the digestion of methylated DNA, leaving only the newly-synthesized mutagenesis product intact, which was then transformed into DH5- α cells. The resulting harvested plasmids were sequenced to confirm the presence of the desired K44A mutation.

The heterodimeric linked L-protein construct in which just one ATPase site received the Walker A K44A mutation was prepared similarly to the non-mutant linked dimer. The mutagenesis reaction was performed again in the same manner as described above, but the reaction used the RSF-duet vector containing the L₁ construct, with the stop codon removed to ensure proper read-through upon translation to yield an appropriate product. The same primers were used in the mutagenesis reaction to achieve the K44A mutation on the L₁ gene. After the resulting plasmid was sequence verified, it was treated with the BamHI and NdeI restriction enzymes for appropriate insertion into the *BchL₂*-containing RSF-duet vector, which received identical treatment with enzyme. Upon DNA harvesting following transformation into DH5- α cells, the resultant constructs were digested with BamHI and KpnI restriction enzymes to verify the presence of both L₁-L₂ inserts, with the *BchL₁* gene containing the desired Walker A mutation.

Expression and Cluster Formation of the Homodimeric Linked L-Protein

The expression vector which contains both the *BchL₁* and *BchL₂* genes was transformed into chemically competent BL21+ *E. coli* cells and cultured on LB agar

plates containing 50 µg/mL kanamycin and 0.34 µg/mL chloramphenicol to ensure plasmid retention. The transformation was accomplished by incubating the BL21+ cells with 0.5 µL of the recovered plasmid DNA. The incubation lasted 20 minutes on ice, after which it was subjected to heat shock treatment by placing the transformation into a water bath at 42°C for 55 seconds. Post-heat shock, the transformation was incubated on ice for an additional 2 minutes prior to the addition of 250 µL LB media. This mixture was incubated at 37°C for 30-45 minutes. The entire volume of the transformation was then plated on the previously mentioned LB agar plates for colony formation and incubated at 37°C overnight.

Post-incubation, a single colony was used to inoculate 5-25 mL LB broth containing 50 µg/mL kanamycin and 0.34 µg/mL chloramphenicol, and was left to incubate overnight at 37°C. This culture was used to inoculate 1 L LB broth containing 50 µg/mL kanamycin, 0.34 µg/mL chloramphenicol, 1 mM iron (III) citrate, and 1 mM L-cysteine by adding 1-10 mL from the overnight growth. The growth is monitored stringently via UV/vis spectrophotometer until the absorbance at 578 registers an O.D. = 0.4. At this time, the cultures are shifted from 37°C to 25°C. When the O.D. = 0.5, 50 µM IPTG is added to each flask for the triggering of protein expression. This induction occurs overnight in preparation for cell harvesting and cluster formation.

Cluster formation for the homodimeric linked L-protein follows the same protocol as the wild-type unlinked protein. The IPTG-induced cultures are transferred to 1 L centrifuge bottles and are made reducing by the addition of 2 mM sodium dithionite under atmosphere of nitrogen. These bottles were left to incubate at 17°C for three hours

to facilitate an environment which fosters the formation of the [4Fe-4S] clusters required for catalysis. Following this incubation, the bottles are placed in a centrifuge, and cells are collected by spinning at 5000 rpm for 20 minutes. The cells are re-suspended in buffer containing 100 mM HEPES, 10 mM MgCl₂, and 2 mM dithionite which is then transferred anaerobically via syringe into sealed vials purged of oxygen and equilibrated with nitrogen. The collected cells are placed in -20°C for storage until it becomes necessary to purify the protein.

Growth and Cluster Formation of the Homodimeric Non-linked Walker A Mutant L-Protein

The growth and expression of the non-linked K44A L-protein mutant is identical to that of the wild-type, and homodimeric linked L-proteins, beginning with the transformation of the generated K44A unlinked construct of *BchL* into BL21+ *E. coli* cells, described previously. After a starter culture was made and incubated overnight, 1-10 mL were used to inoculate 1 L LB broth containing 50 µg/mL kanamycin, 100 µg/mL ampicillin, 0.34 µg/mL chloramphenicol, 1 mM iron (III) citrate, and 1 mM L-cysteine. In similar manner to the expression of the aforementioned proteins, the antibiotics ensure plasmid retention throughout the growth process, whereas the iron and cysteine additives, upon anaerobic conditions, become the building blocks for the [4Fe-4S] clusters that are incorporated into the functional protein. In preparation for IPTG induction, the optical density is monitored by spectrophotometer at a wavelength absorbance equal to 578 nm until a reading of 0.4 is achieved. At this juncture, the cultures are shifted from 37°C to 25°C until the O.D. reaches a value of 0.5. This is the point where IPTG is added to a

final concentration of 50 μM to allow for the slow expression of protein overnight. The protocols for anaerobic cluster formation and cell harvesting are identical to the previously mentioned proteins.

Expression and Cluster Formation of the Heterodimeric Linked Walker A Mutant L-Protein

The expression of the heterodimeric linked K44A L-protein variant is based off of the previously mentioned protocols, but deviate slightly due to poor plasmid expression with IPTG induction. As before, the genetic construct containing the heterodimeric linked K44A *BchL* gene in which one ATPase site has been knocked out was transformed into 50 μL BL21+ *E. coli* cells and incubated on ice for 20 minutes. Following this incubation, the cells undergo a heat shock at 42°C for 55 seconds, which allows for the expansion of membrane pores to facilitate successful DNA uptake, followed by incubation on ice for an additional 2 minutes closes the pores to aid in plasmid retention. Following these treatments, the transformation is added to 250 μL of LB media and immediately incubated at 37°C for 30-45 minutes. The entire volume was plated on LB agar plates containing 50 $\mu\text{g}/\text{mL}$ kanamycin, 100 $\mu\text{g}/\text{mL}$ ampicillin, and 0.34 $\mu\text{g}/\text{mL}$ chloramphenicol. These plates are incubated overnight at 37°C, which upon successful colony formation, becomes the inoculant for 5-50 mL of starter culture in preparation for large-scale growth and expression of protein.

A volume of 1-25 mL from the overnight starter culture is used to inoculate 1 L flasks containing LB broth, 50 $\mu\text{g}/\text{mL}$ kanamycin, 100 $\mu\text{g}/\text{mL}$ ampicillin, 0.34 $\mu\text{g}/\text{mL}$ chloramphenicol, 1 mM iron (III) citrate, and 1 mM L-cysteine. Due to a slow growth

phase, a higher volume of starter culture was used. The deviations from the wild-type, and previous L-protein derivative growth and expression protocols include monitoring the optical density while incubating at 37°C until a reading of 0.6 is registered via spectrophotometer set to read wavelength absorbance at 600 nm. At this point, IPTG is added to each flask to a final concentration of 0.5 mM to induce protein expression. The flasks are left to incubate for 3 hours at 37°C, prior to collection in 1 L centrifuge bottles. To the cells, 2 mM dithionite is added to create a reducing environment conducive for cluster formation. The sealed bottles are placed in an incubator set to 17°C for three hours before cell collection by centrifuge at 5000 rpm for 20 minutes. The supernatant is carefully decanted under atmosphere of nitrogen, and the resulting cell pellet is re-suspended in buffer containing 100 mM HEPES, 10 mM MgCl₂, and 2 mM dithionite before transferring anaerobically via syringe into a sealed vial purged of oxygen and equilibrated with nitrogen. The cells are then frozen and stored at -20°C in preparation for purifying the protein contained within.

Purification of the L-Protein Variants

Due to the similarity in nature of each of the generated L-protein variants, their purification strategy was based off of the wild-type purification. The previously harvested cells were taken from storage at -20°C and placed in a water bath at room temperature to thaw out while maintaining an atmosphere of nitrogen. During the thawing process, equilibration buffer containing 100 mM HEPES pH 7.5, and 150 mM NaCl was degassed using a vacuum manifold and replacing the atmosphere with nitrogen in consecutive cycles. Following degasification, the buffer was reduced by the addition of 2 mM

dithionite. A French pressure cell was used to lyse the cells using an adapted protocol to ensure that an anaerobic environment was maintained to protect the oxygen-labile metal clusters that were incorporated into the proteins. This was accomplished by placing needles on the in and out lines of the pressure cell for the loading and collection of the cell lysate, and a constant stream of nitrogen was maintained during cell lysis. Prior to the addition of the thawed cells, 30 mL reduced equilibration buffer was passed through to generate a reducing environment within the apparatus. Following cell lysis, the total cell lysate was transferred anaerobically by syringe into centrifuge tubes that have been equilibrated with nitrogen. Clarification of the lysate was accomplished by centrifugation at 17000 rpm for 1 hour to separate both the soluble and insoluble fractions. The resulting supernatant was carefully transferred into an empty, degassed vial containing dilution buffer consisting of 0.7 mL 1 M HEPES pH 7.5, 2.3 mL H₂O, and 350 mg NaCl in preparation for loading onto a Ni-NTA column.

The column is made reducing by passing degassed, reducing equilibration buffer until a positive colorimetric result is obtained when the flow-through yields a positive result by using methyl viologen as an indicator. The protein is then loaded onto the Ni-column and washed with buffer containing 100 mM HEPES pH 7.5, 150 mM NaCl, and 20 mM imidazole, made reducing with the addition of 2 mM dithionite. Because the proteins contain [4Fe-4S] clusters as an essential part of their composition, evidence that the protein has bound to the column is indicated by the appearance and retention of a dark brown band both during and after passing wash buffer through the column. Following the washing step, elution buffer was passed through the column which contains 250 mM

imidazole. The migrating band at this step is collected in an empty sealed, degassed vial. The homodimeric linked L-protein, and the non-linked K44A dual ATPase mutant L-protein were added to a dilution buffer containing 100 mM HEPES pH 7.5, 200 mM NaCl, and 2 mM dithionite before concentration using a 30 kDa cut-off filter. The concentration apparatus is made reducing by passing a portion of the reduced dilution buffer, followed by the addition of protein. Following the concentration of protein, the collected portion was pelleted, collected, and stored in liquid nitrogen in preparation for *in vitro* characterization.

The heterodimeric single K44A linked L-protein was subjected to an additional purification step following Ni-elution. Instead of eluting into a dilution buffer containing 200 mM NaCl, the protein was instead added to buffer containing no salt in preparation for addition to a Q-sepharose column. To prepare the Q-column for addition of protein, the resin was pre-washed using a 1 M salt solution which was first degassed and reduced with 2 mM dithionite. The column was then rinsed with degassed and reduced buffer containing no salt to promote protein binding to the column during loading, again indicate by dark brown discoloration. Following the addition of protein, the column was washed with 10% salt solution, and then eluted using a NaCl gradient, from 20%-45%. The heterodimeric single K44A linked L-protein will elute beginning at around the 35% salt mark. The elutant is collected in sealed, degassed, and empty vials in preparation for concentration, described previously.

*Tev Protease Cleavage of the Homodimeric Linked L-Protein and Pchlde Reduction
Endpoint Assays*

In preparation for the *in vitro* characterization of each of the purified L-protein variants with the remaining DPOR components, the homodimeric linked L-protein was subjected to treatment with *AcTev* protease (Thermo Fisher Scientific) by incubating 10 μ L of the purified linked homodimer with 20 units protease, and made up to 30 μ L using buffer containing 100 mM HEPES pH 7.5, 10 mM $MgCl_2$, and 2 mM dithionite. The reactions were performed in Eppendorf tubes contained in sealed, degassed vials under a constant stream of nitrogen. The wild-type L-protein also underwent this treatment as a control, with the results monitored by SDS-PAGE (Figure 3.3B). Following this cleavage, Pchlde reduction endpoint assays were performed using both uncleaved and cleaved homodimeric linked L-protein, in addition to the dual and single Walker A mutant L-proteins, using the wild-type construct as a positive control. A negative control using the wild-type DPOR system, but no ATP was also tested.

Reaction buffer was prepared that contained 50 mM HEPES pH 7.5, 10 mM $MgCl_2$, and 6 mM dithionite that was sealed in a crimp-shut vial and purged of oxygen. Each protein was taken from storage in liquid nitrogen and immediately placed on vacuum manifold for degasification. The Pchlde and ATP used in the reactions were similarly degassed under vacuum. The reaction components were then added to the following concentrations: 2 μ M NB, 8 μ M L (or respective variant), and 10 μ M Pchlde. The reactions were brought up to a final volume of 500 μ L using the degassed, reducing reaction buffer. Each reaction was initiated separately by the addition of 2 mM degassed

ATP, with the exception of the no-ATP negative control, mixing with the syringe to ensure a homogeneous mixture throughout. After 10 or 30 minutes, the reactions were quenched by removing 200 μL from the reaction mixture and placing in 800 μL 100% v/v acetone, which serves to precipitate the protein components, suspending the Pchl_{ide}/Chl_{ide} mixture in the organic phase. This mixture was harvested by centrifuge at 13000 rpm for 10 minutes, where they were subjected to spectroscopic analysis by measuring absorbance profiles over a wavelength range of 700-580 nm for each assay condition.

Real-time Pchl_{ide} Kinetic Assay Using the Homodimeric Linked L-Protein

To better characterize the homodimeric linked L-protein with respect to the native L-protein, kinetic assays were established that monitored the rate of Chl_{ide} formation in real time using the absorbance value of 675 nm via spectrometer, indicative of reduced substrate. Reaction buffer containing 100 mM HEPES pH 7.5, 10 mM MgCl₂, and 6 mM dithionite was prepared and degassed by placing onto vacuum manifold and switching to steady nitrogen flow in alternating cycles. Separate empty vials containing small Eppendorf tubes were degassed in preparation for mixing each reaction. The DPOR protein components were taken from storage and degassed immediately to protect the oxygen-labile metal centers.

Following degasification, each component was added as follows to make the wild-type condition: 25 μM Pchl_{ide}, 8 μM NB, 32 μM L, adding reaction buffer to obtain a final volume of 600 μL to achieve the desired concentrations. A similar reaction condition was established which included the homodimeric linked L-protein in place of

the native construct, as well as a negative control which included the wild-type DPOR components, but was not introduced to ATP. The reaction mixtures were each placed into a sealed, degassed cuvette containing a nitrogen atmosphere and placed into the spectrophotometer prior to reaction initiation. Each reaction was initiated by the addition of 5 mM ATP and immediately mixed and monitored at 675 nm with data points being continuously collected over the course of 10 minutes.

3.3 RESULTS

Cloning and Expression of L-Protein Variants

In preparation for intensive studying with regard to the dynamic role ATP hydrolysis in the L-protein seems to have in DPOR mediated Pchlide reduction, genetic constructs encoding for a homodimeric linked L-protein, in addition to two novel ATP variants—one a homodimeric K44A Walker A non-linked mutant, and the other a heterodimeric linked construct in which only one monomer of the L-protein contains the K44A mutation—were generated successfully and appear to encode for the appropriate gene products when expressed in the *BL21+* expression system under IPTG induction (Figure 3.3A). When using the purification method developed for the isolation of the wild-type DPOR components adapted to the L-protein variants listed above, the resulting proteins appear to be greater than 95% pure, with the exception of the heterodimeric K44A Walker A L-protein. While the protein is expressed well using the previously mentioned protocol alterations, the resulting protein isolate after purification contains contaminants that are not seen in the wild-type, or other variants column elutants, even when adding the Q-sepharose polishing step.

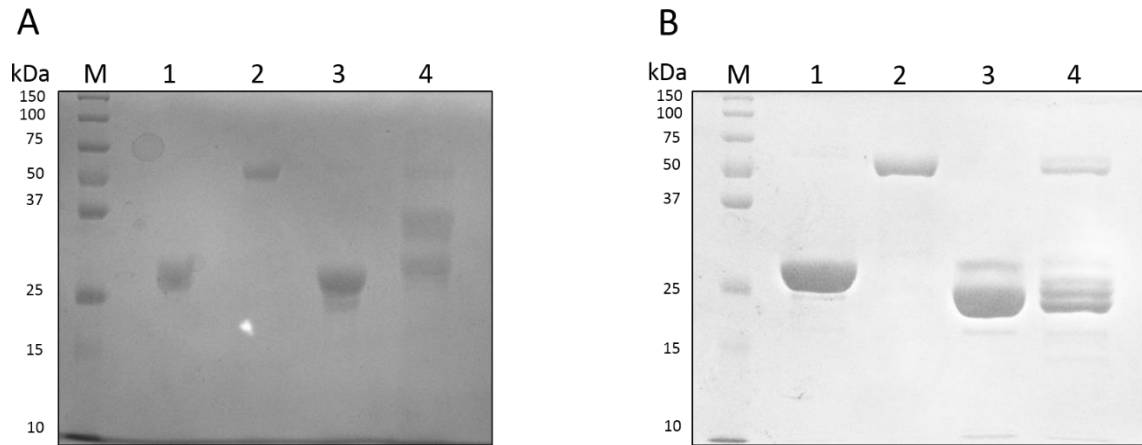


Figure 3.3. Depiction of purified L-protein variants by SDS-PAGE. (A) Analysis of purified L-proteins. SDS-PAGE depiction of purified L-protein constructs, analyzed on a 10% gel. Lane 1, wild-type BchL; Lane 2, homodimeric linked BchL; Lane 3, homodimeric K44A BchL; Lane 4, heterodimeric K44A linked BchL. The molecular weight for un-linked BchL constructs is 32 kDa, and 64 kDa for linked constructs. (B) *Tev* cleavage of the homodimeric linked L-protein. Purified linked BchL was incubated with 20 units of *AcTev* protease for 1 hour in tandem with the wild-type construct to observe the formation of appropriately sized products in preparation for use in Pchlide reduction assays, also monitored on a 10% SDS-PAGE. Lane 1, wild-type BchL; Lane 2, linked BchL; Lane 3, wild-type BchL incubated with *tev* protease; Lane 4, linked BchL incubated with *tev* protease.

The Homodimeric Linked L-Protein Behaves Similarly to the Wild-type Construct

With the successful isolation of the homodimeric linked L-protein, the next step was to assay its influence on the DPOR system when introduced in place of the native L-protein. With regard to its ability to promote substrate reduction, qualitatively speaking, we observed the reduction of Pchlide to Chlide, which was evidenced by a spectral shift from 626 nm to 665 nm from the acetone extracted assay products (Figure 3.4). The amount of Pchlide reduction seen in the wild-type and the linked systems appears to be

quite similar. Interestingly, the state of the linking unit between monomers does not appear to affect substrate reduction, as evidenced by the fact that similar Chlide formation profiles were obtained when the intact linked L-protein was used, as well as with the *tev* protease-treated protein as well. Quantitatively, the kinetic data for Pchlde reduction reveals that the linked L-protein construct is capable of facilitating a rate of Chlide formation that is highly reminiscent with what is observed in the native system. When the linked L-protein was used, substrate reduction occurred at a rate of 2.13×10^{-6} M minute⁻¹, compared to the similar rate of 2.68×10^{-6} M minute⁻¹ in the native DPOR system (Figure 3.5).

The Walker A L-Protein Mutants Are Incapable of Substrate Reduction

Structural data suggests that the lysine 44 of the L-protein from *Rhodobacter sphaeroides* is part of the Walker A motif crucial for ATPase activity⁶. While the homodimeric linked L-protein showed sufficient ability to work with the NB-protein to accomplish substrate reduction, the novel Walker A altered variants in which Lys44 was replaced with alanine did not. The Pchlde reduction assay data suggest that after 10 minutes, there was no observable conversion of Pchlde to Chlide (Figure 3.4). Even when the length of the reaction was increased to more than 30 minutes, there was still no substrate reduction observed. It also appears that both ATPase sites are required for appropriate catalysis, evidenced by the fact that both the homodimeric K44A mutant, as well as the heterodimeric K44A linked construct were incapable of producing Chlide *in vitro* with ATP present.

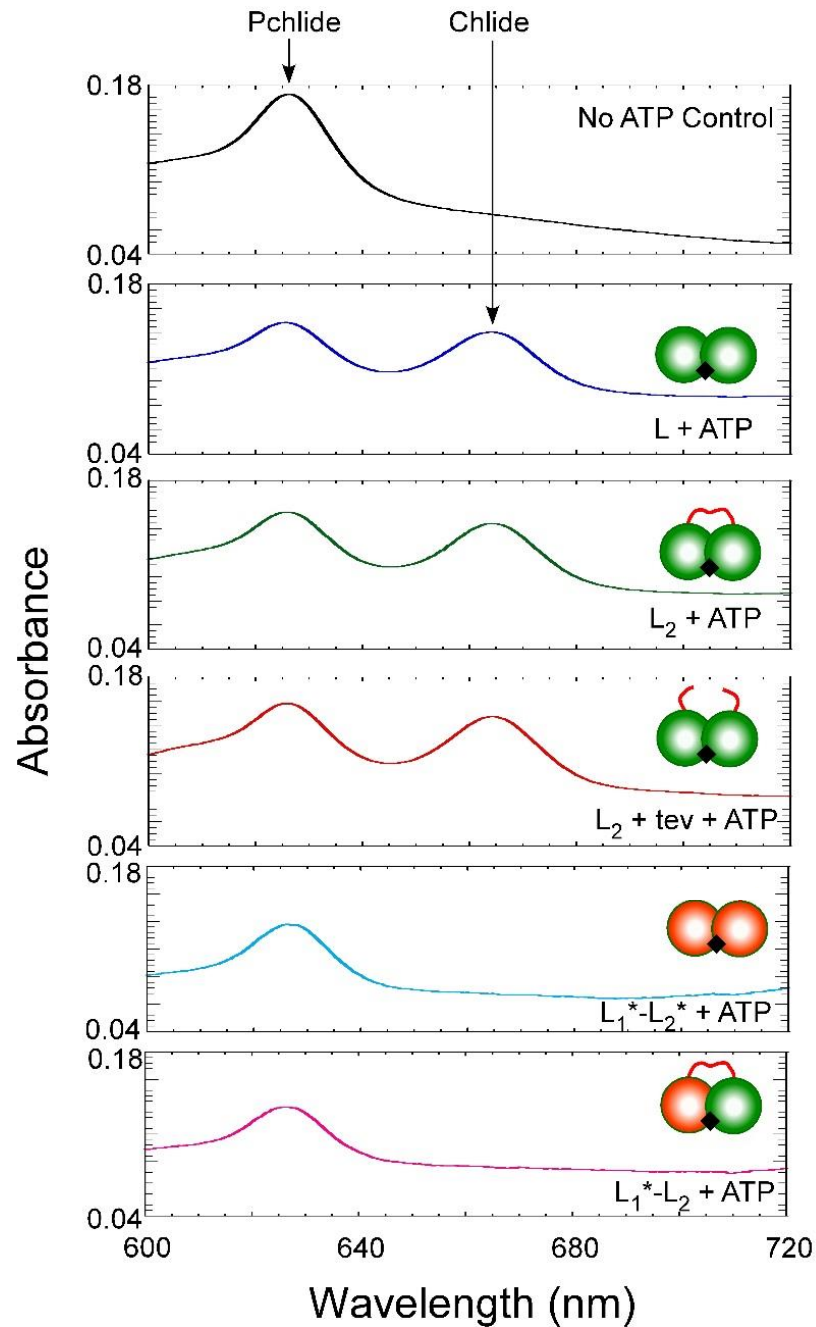


Figure 3.4. Qualitative Pchlride reduction scans. Each L-protein construct was incubated together with BchNB, Pchlride, and ATP to observe either the capability or inability to accomplish substrate reduction. The L-protein constructs that were successful in reducing Pchlride to Chlide were those that did not carry the K44A mutation, including the linked L-protein that was not treated with protease. The constructs that harbored a mutation in the Walker A motif were unable to produce Chlide, evidenced by an emergence of a wavelength absorbance peak at 665 nm.

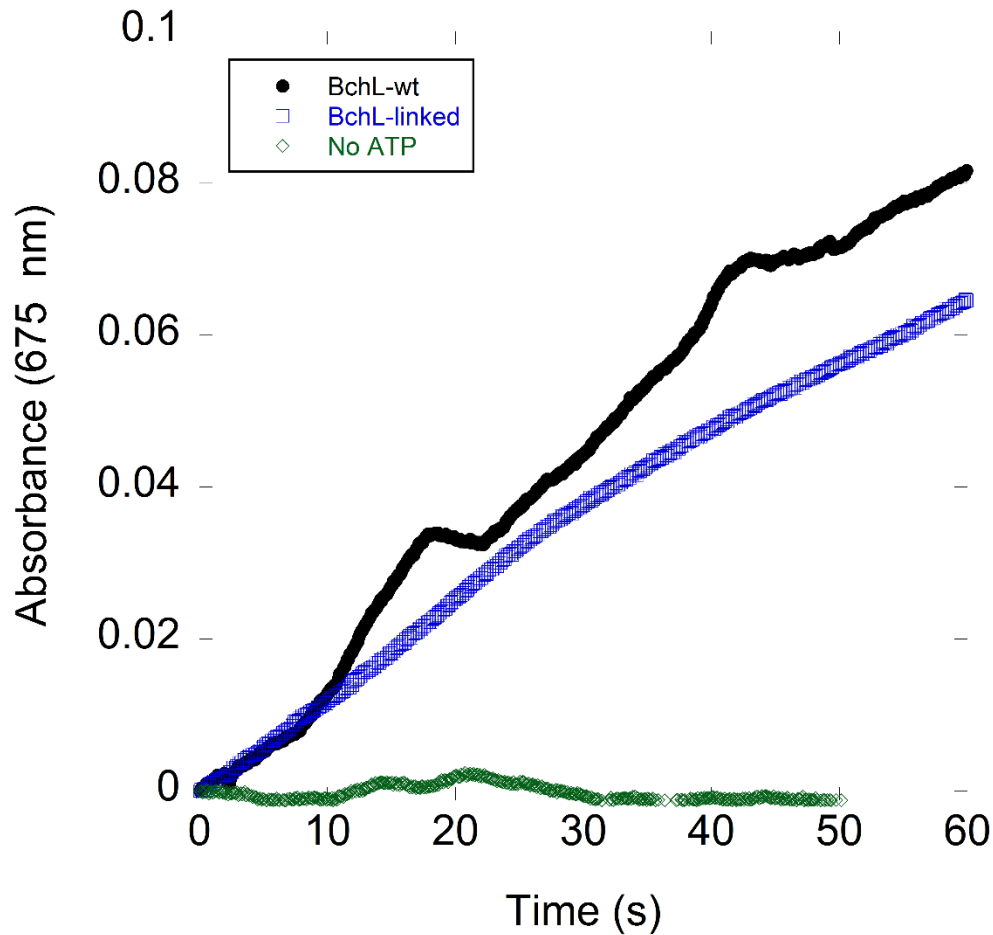


Figure 3.5. Wild-type BchL and homodimeric linked L-protein reduction kinetics. As measured by real-time Chlide formation assays, both the wild-type L-protein and the linked construct were capable of substrate reduction when incubated with wild-type NB-protein in standard reaction conditions, as evidenced by the appearance of an absorbance maximum at 675 nm, which is indicative of the formation of Chlide. Interestingly, the kinetics of both wild-type, and linked construct reactions were similar when incubated with 5 mM ATP, indicating that the linked construct has function that is analogous to the wild-type protein *in vitro*, and is sufficient to promote substrate reduction.

3.4 DISCUSSION

Studies from nitrogenase, due to their similar subunit architecture and method of substrate reduction, are helpful in elucidating interesting characteristics of how DPOR may function to act to reduce Pchlide to Chlide. Like nitrogenase, the binding of ATP is an integral step during catalysis. To gain insight into how this process affects DPOR function, we generated a series of constructs that aimed to highlight the dynamics of the L-protein during ATP binding and hydrolysis. First, a homodimeric linked L-protein construct was created that was found to behave favorably when replacing the wild-type protein in the native DPOR system. This is critical because for any future studies directed at studying L-protein dynamics, such as observing and characterizing the putative rolling motion of the L-protein, based on similar observations in nitrogenase¹, and how the binding and hydrolysis of ATP may facilitate this motion, the generated homodimer must behave in a similar manner to the wild-type construct for any conclusions to be met with any degree of confidence.

The fact that we observed such similarity between the linked L-protein and the native construct is promising, and establishes precedent for future research to be accomplished in this area. The fact that both ATP are necessary for catalysis is equally intriguing. The fact that the singly-mutated linked L-protein was completely incapable of substrate reduction, even though one ATPase site is still fully capable of ATP binding and hydrolysis suggests that it is only when ATP is bound to both monomeric units that a catalytically relevant complex is formed to facilitate in the necessary electron transfer and ATP hydrolysis required to produce Chlide. It will be interesting to note in future

research if this singly-mutated L-protein construct is capable of ATP hydrolysis, or if that too is reliant upon the other ATPase site for proper function. Before that avenue is to be explored, the protocols detailing the construction, expression, and purification of the L-protein K44A heterodimer will need to be optimized in order to obtain enough protein to properly characterize its function. In any case, the generation and initial characterization of all L-protein constructs described in this chapter provide a richer understanding in how the utilization of ATP affects DPOR function, as well as provides a basis for future research capable of yielding even greater insight about the enzymology of Pchlide reduction.

REFERENCES

1. Tezcan, F. A., Kaiser, J. T., Mustafi, D., Walton, M. Y., Howard, J. B., Rees, D. C. Nitrogenase complexes: multiple docking sites for a nucleotide switch protein. *Science* **309** (5739), 1377-80 (2005).
2. Walker, J. E., Saraste, M.; Runswick, M. J., Gay, N. J. Distantly related sequences in the alpha- and beta-subunits of ATP synthase, myosin, kinases and other ATP-requiring enzymes and a common nucleotide binding fold. *Embo j* **1** (8), 945-51 (1982).
3. Seefeldt, L. C., Morgan, T. V., Dean, D. R., Mortenson, L. E. Mapping the site(s) of MgATP and MgADP interaction with the nitrogenase of *Azotobacter vinelandii*. Lysine 15 of the iron protein plays a major role in MgATP interaction. *J Biol Chem* **267** (10), 6680-8 (1992).
4. Ryle, M. J., Seefeldt, L. C. Elucidation of a MgATP signal transduction pathway in the nitrogenase iron protein: formation of a conformation resembling the MgATP-bound state by protein engineering. *Biochemistry* **35** (15), 4766-75 (1996).
5. Mortenson, L. E., Seefeldt, L. C., Morgan, T. V., Bolin, J. T. The role of metal clusters and MgATP in nitrogenase catalysis. *Adv Enzymol Relat Areas Mol Biol* **67**, 299-374 (1993).
6. Sarma, R., Barney, B. M., Hamilton, T. L., Jones, A., Seefeldt, L. C., Peters, J. W. Crystal structure of the L protein of *Rhodobacter sphaeroides* light-independent protochlorophyllide reductase with MgADP bound: a homologue of the nitrogenase Fe protein. *Biochemistry* **47** (49), 13004-15 (2008).

SUMMARY AND FUTURE WORK

Chlorophyll is an essential component in the capture and conversion of light energy during photosynthesis to accomplish cellular work. The synthetic pathway of active chlorophyll is highlighted by the two-electron reduction of Pchlide to generate Chlide, the immediate precursor to chlorophyll *a*¹. Angiosperms have developed a sensing mechanism that detects levels of Pchlide to protect itself from accumulation of ROS damage². More broadly speaking, the conversion of Pchlide to Chlide serves as the rate-limiting step during chlorophyll synthesis³. The focus of this thesis was to highlight the dynamic role that ATP plays during the DPOR-mediated reduction of Pchlide to Chlide in the chlorophyll synthetic pathway.

DPOR is structurally similar to the enzyme nitrogenase⁴. The similarity is most apparent when looking at the L-protein of DPOR and the Fe-protein of nitrogenase⁵, but the overall subunit topology is striking between the two systems, consisting of two symmetrical catalytic halves which are reliant on the binding and hydrolysis of ATP to accomplish substrate reduction⁶. In DPOR, a similar ATP requirement is needed to coordinate events including electron transfer, and subunit dissociation for each catalytic half of the functional complex. Recent discoveries give insight to how, and when these events occur in the nitrogenase system—that ATP hydrolysis occurs post electron transfer⁷, and that these hydrolysis events potentially highlight an alternating catalysis model which involves allosteric crosstalk between catalytic halves. When similar kinetic studies were accomplished, a number of interesting findings were made, particularly

when compared with what is now known about nitrogenase. First, the steady-state rate for ATP hydrolysis occurs 400 fold more slowly in DPOR than in nitrogenase. Interestingly, the preliminary pre-steady state characterization of catalytic events discussed in Chapter II show that the initial burst rate for ATP hydrolysis in DPOR matches the rate that is observed in nitrogenase (73 second^{-1} and 70 second^{-1} , respectively), however, the release of phosphate post-hydrolysis occurs much more slowly. Further studies detailing structural differences and mutational studies addressing the discrepancy observed between rate constants may help to glean understanding as to why similarly constructed ATPase motors behave so drastically different kinetically. Indeed, the elucidation of additional first-order rate constants, such as those for ADP-release and subunit dissociation of the L-protein from the NB-protein post-hydrolysis may give additional insight into the catalytic mechanism of the single-electron transferring cycle that occurs in DPOR.

In addition to the kinetic characterization of the ATP-mediated L-protein cycle described above, and in detail in Chapter II, novel L-protein constructs were created to illuminate the dynamics that occur during catalysis. In nitrogenase, evidence shows that there are distinct Fe-protein docking states on the MoFe-protein depending on the state of nucleotide which is bound to the Fe-protein⁸, which points to a rolling motion during catalysis. Additional mutational studies that affect the ability of the Fe-protein to bind and hydrolyze ATP abolish normal function with respect to substrate reduction⁹. The studies mentioned in Chapter III confirm the essential role of ATP during catalysis, as

well as describe the construction of a linked L-protein that appears to function similarly to the wild-type construct.

These exciting data show that the L-protein may be expressed and purified as a single polypeptide, and that the linked construct is capable of substrate reduction in a manner that is both qualitatively and kinetically similar to the wild-type construct when incubated with the native DPOR system. Additionally, we show that both ATPase sites are required for function, and when one, or both of the sites are affected, a loss of function is observed. In the future, the role of each ATPase site may be further characterized by using the Walker A mutants to assess their ability to hydrolyze ATP, and how that affects substrate reduction. For this to happen, the expression and purification of the heterodimeric K44A linked L-protein will need to be optimized for confident characterization.

Furthermore, additional work may be done with the homodimeric L-protein construct with respect to fluorescent labelling. Site-specific labelling of the L-protein may be accomplished on the linked construct using unnatural amino acid incorporation coupled with click chemistry to attach a fluorophore on a position that will allow for observation of the rate of ATPase-dependent rolling during catalysis. For this to become possible, additional linked constructs of the NB-protein will have to be generated, also labelled with fluorophore in a similar manner. Using Forster Resonance Energy Transfer (FRET) techniques, both the rate of the rolling motion will be captured, as well as rates for subunit dissociation during the L-protein cycle. Furthermore, the linked NB-protein construct may be similarly modified to render only one active site inert by site-directed

mutagenesis. This may be accomplished by the mutation of the BchB'-Asp274 to an alanine, as substrate reduction is not observed in these constructs⁶. By generating a single-site NB-protein mutant, as described above, it may become possible to observe further evidence that both catalytic halves communicate in an allosteric manner to coordinate events regarding the L-protein cycle, as well as substrate reduction.

As currently constituted, the investigation outlined in the preceding chapters serves to establish what is currently known about the DPOR-mediated conversion of Pchl_{id} to Chl_{id} during chlorophyll biosynthesis, the characterization of wild-type ATPase activity with regards to kinetic characterization of events in the catalytic mechanism of the L-protein, and how alterations in one or both of the ATPase sites affect the ability of the L-protein to function with respect to substrate reduction. While a number of questions still remain concerning DPOR function, the future work described above may assist in uncovering additional information with respect to the mechanics on how DPOR functions during chlorophyll biosynthesis.

REFERENCES

1. Von Wettstein, D., Gough, S., Kannangara, C. G. Chlorophyll Biosynthesis. *Plant Cell* **7** (7), 1039-1057 (1995).
2. Reinbothe, S., Reinbothe, C., Apel, K., Lebedev, N. Evolution of chlorophyll biosynthesis--the challenge to survive photooxidation. *Cell* **86** (5), 703-5 (1996).
3. Masuda, T., Fujita, Y. Regulation and evolution of chlorophyll metabolism. *Photochem Photobiol Sci* **7** (10), 1131-49 (2008).
4. Moser, J., Lange, C., Krausze, J., Rebelein, J., Schubert, W. D., Ribbe, M. W., Heinz, D. W., Jahn, D. Structure of ADP-aluminium fluoride-stabilized protochlorophyllide oxidoreductase complex. *Proc Natl Acad Sci U S A* **110** (6), 2094-8 (2013).
5. Sarma, R., Barney, B. M., Hamilton, T. L., Jones, A., Seefeldt, L. C., Peters, J. W. Crystal structure of the L protein of *Rhodobacter sphaeroides* light-independent

protochlorophyllide reductase with MgADP bound: a homologue of the nitrogenase Fe protein. *Biochemistry* **47** (49), 13004-15 (2008).

6. Muraki, N., Nomata, J., Ebata, K., Mizoguchi, T., Shiba, T., Tamiaki, H., Kurisu, G., Fujita, Y. X-ray crystal structure of the light-independent protochlorophyllide reductase. *Nature* **465** (7294), 110-4 (2010).

7. Duval, S., Danyal, K., Shaw, S., Lytle, A. K., Dean, D. R., Hoffman, B. M., Antony, E., Seefeldt, L. C. Electron transfer precedes ATP hydrolysis during nitrogenase catalysis. *Proc Natl Acad Sci U S A* **110** (41), 16414-9 (2013).

8. Tezcan, F. A., Kaiser, J. T., Mustafi, D., Walton, M. Y., Howard, J. B., Rees, D. C. Nitrogenase complexes: multiple docking sites for a nucleotide switch protein. *Science* **309** (5739), 1377-80 (2005).

9. Seefeldt, L. C., Morgan, T. V., Dean, D. R., Mortenson, L. E. Mapping the site(s) of MgATP and MgADP interaction with the nitrogenase of *Azotobacter vinelandii*. Lysine 15 of the iron protein plays a major role in MgATP interaction. *J Biol Chem* **267** (10), 6680-8 (1992).